

DTIC FILE COPY

(24)

USAFSAM-TP-90-17

AD-A231 230

**PROTON DEPTH DOSE DISTRIBUTION: 3-D
CALCULATION OF DOSE DISTRIBUTIONS
FROM SOLAR FLARE IRRADIATION**

Dennis D. Leavitt, Ph.D.

DTIC
ELECTE
JAN 23 1991
S D D

**Texas A&M Research Foundation, Inc.
Box 3578
College Station, TX 77843**

November 1990

Interim Report for Period May 1988 - November 1988

Approved for public release; distribution is unlimited.

**Prepared for
USAF SCHOOL OF AEROSPACE MEDICINE
Human Systems Division (AFSC)
Brooks Air Force Base, TX 78235-5301**



01 1 22 072

NOTICES

This interim report was submitted by Texas A&M Research Foundation, Inc., Box 3578, College Station, Texas, under contract F33615-87-D-0627/0005, job order 7757-04-41, with the USAF School of Aerospace Medicine, Human Systems Division, AFSC, Brooks Air Force Base, Texas. Mr. Kenneth A. Hardy (USAFSAM/RZB) was the Laboratory Project Scientist-in-Charge.

When Government drawings, specifications, or other data are used for any purpose other than in connection with a definitely Government-related procurement, the United States Government incurs no responsibility or any obligation whatsoever. The fact that the Government may have formulated or in any way supplied the said drawings, specifications, or other data, is not to be regarded by implication, or otherwise in any manner construed, as licensing the holder or any other person or corporation; or as conveying any rights or permission to manufacture, use, or sell any patented invention that may in any way be related thereto.

The Office of Public Affairs has reviewed this report, and it is releasable to the National Technical Information Service, where it will be available to the general public including foreign nationals.

This report has been reviewed and is approved for publication.

Kenneth A. Hardy
KENNETH A. HARDY, M.S.
Project Scientist

Stanley L. Hartgraves
STANLEY L. HARTGRAVES, Lt Col, USAF, BSC
Supervisor

George E. Schwender MD
GEORGE E. SCHWENDER, Colonel, USAF, MC, CFS
Commander

UNCLASSIFIED

SECURITY CLASSIFICATION OF THIS PAGE

REPORT DOCUMENTATION PAGE

Form Approved
OMB No. 0704-0188

1a. REPORT SECURITY CLASSIFICATION Unclassified		1b. RESTRICTIVE MARKINGS		
2a. SECURITY CLASSIFICATION AUTHORITY		3. DISTRIBUTION/AVAILABILITY OF REPORT Approved for public release; distribution is unlimited. ✓		
2b. DECLASSIFICATION/DOWNGRADING SCHEDULE				
4. PERFORMING ORGANIZATION REPORT NUMBER(S)		5. MONITORING ORGANIZATION REPORT NUMBER(S) USAFSAM-TP-90-17		
6a. NAME OF PERFORMING ORGANIZATION Texas A&M Research Foundation Inc.	6b. OFFICE SYMBOL (if applicable)	7a. NAME OF MONITORING ORGANIZATION USAF School of Aerospace Medicine (RZB)		
6c. ADDRESS (City, State, and ZIP Code) Box 3578 College Station, TX 77843		7b. ADDRESS (City, State, and ZIP Code) Human Systems Division (AFSC) Brooks Air Force Base, TX 78235-5301		
8a. NAME OF FUNDING/SPONSORING ORGANIZATION	8b. OFFICE SYMBOL (if applicable)	9. PROCUREMENT INSTRUMENT IDENTIFICATION NUMBER F33615-87-D-0627/0005		
8c. ADDRESS (City, State, and ZIP Code)		10. SOURCE OF FUNDING NUMBERS		
		PROGRAM ELEMENT NO. 62202F	PROJECT NO. 7757	TASK NO. 04
11. TITLE (Include Security Classification) Proton Depth Dose Distribution: 3-D Calculation of Dose Distributions from Solar Flare Irradiation				
12. PERSONAL AUTHOR(S) Leavitt, Dennis D.				
13a. TYPE OF REPORT Interim	13b. TIME COVERED FROM 88/5/01 TO 88/11/17	14. DATE OF REPORT (Year, Month, Day) 1990, November	15. PAGE COUNT 40	
16. SUPPLEMENTARY NOTATION				
17. COSATI CODES		18. SUBJECT TERMS (Continue on reverse if necessary and identify by block number) Depth dose distribution; Solar flare protons; Radiation dosimetry space radiation. ✓		
FIELD	GROUP			SUB-GROUP
06	07			
03	02			
19. ABSTRACT (Continue on reverse if necessary and identify by block number) Relative depth dose distribution to the head from 3 typical solar flare proton events were calculated for 3 different exposure geometries: (1) single directional radiation incident upon a fixed head; (2) single directional radiation incident upon head rotating axially (2-D rotation); and (3) omnidirectional radiation incident upon head (3-D rotation). Isodose distributions in the transverse plane intersecting isocenter are presented for each of the 3 solar flare events in all 3 exposure geometries. In all 3 calculation configurations the maximum predicted dose occurred on the surface of the head. The dose at the isocenter of the head relative to the surface dose for the 2-D and 3-D rotation geometries ranged from 2% to 19%, increasing with increasing energy of the event. The calculations suggest the superficially located organs (lens of the eye and skin) are at greatest risk for the proton events studied here. (25) * Solar flares, * Irradiation * Dosimetry,				
20. DISTRIBUTION/AVAILABILITY OF ABSTRACT <input checked="" type="checkbox"/> UNCLASSIFIED/UNLIMITED <input type="checkbox"/> SAME AS RPT <input type="checkbox"/> DTIC USERS		21. ABSTRACT SECURITY CLASSIFICATION Unclassified		
22a. NAME OF RESPONSIBLE INDIVIDUAL Kenneth A. Hardy		22b. TELEPHONE (Include Area Code) (512) 536-3417	22c. OFFICE SYMBOL USAFSAM/RZB	

PURPOSE

approximately
d
0-38.

polar
10% dose
Mullen,
e
o.3, June

Boxes

u/or
special

Dist

A-1

CALCULATION TECHNIQUE

An existing clinical radiation therapy treatment planning program was used to calculate the single fixed field isodose distributions and the 2-D rotational isodose distributions. A 3-D dose calculation program was written to calculate the 3-D isodose distributions. Key points of the dose calculation program for all 3 cases are:

1. All isodose distributions are displayed relative to a normalization dose of 100 centigray at the isocenter in the absence of the head phantom.

2. The incident beam profile is assumed to be uniform (no variation in intensity across the field in a direction perpendicular to the incident ray).

3. Effective source position for all calculations set to 1,000 cm (this simulates a planar field with only minimum divergence).

4. The head phantom is assumed to be of unit density (no correction for increased density of skull).

5. Tissue absorption effects are calculated by determining the ray path length through the head phantom to the calculation point. The ray originates at the effective source position (1,000 cm from isocenter) and continues through the calculation point. The typical path length through the head phantom to isocenter ranges from 7 cm to 12 cm, while the path length for points on the surface of the phantom is zero for beams incident on that surface and may be as much as 20 cm to that same point for beams incident on the opposite side of the head.

6. An inverse-square correction is included for all calculation points. For a calculation point at isocenter, this factor is 1.0; for a point 10-cm "upstream" from isocenter relative to a fixed field, this factor is $(1,000/990)^2$, or 1.01; for a point 10cm "downstream" from isocenter relative to a fixed field, this factor is $(1,000/1,010)^2$, or 0.98.

7. Doses for the single fixed field and 2-D rotations are calculated using a dose grid of approximately 9,500 points, while doses for the 3-D rotations are calculated using a dose grid of approximately 4,900 points.

8. Angular increment for the 2-D rotation is set to 3 degrees; the angular increment for the 3-D rotation is set to 20 degrees and the entire rotation is simulated by 14 arc segments equally distributed over the head. Total dose to a calculation point is the sum of dose contributions from each increment. The individual weight applied to the dose from each increment is $(1/(\text{total number of arc increments}))$.

9. Depth dose data are tabulated in 2.5-mm increments to a depth of 10 cm. For depths greater than 10 cm, calculations are based on logarithmic extrapolation from the last two points in the depth dose table.

VERIFICATION OF CALCULATIONS

The 3-D dose calculation program was intercompared with a similar program in use at the Joint Center for Radiation Therapy, Harvard Medical School, Boston, Mass. This intercomparison, using the same data set for the head phantom contours and the same data set for the solar flare depth doses, showed that the isodose distributions resulting from calculations on the 2 independently developed systems agreed to within the thickness of the isodose line. Additionally, the depth dose distributions corresponding to 2-D rotation were calculated for a 10-cm diameter cylinder and compared with the rotated depth doses reported for simulated solar proton events of 10 July 1959 and 23 February 1956. This comparison revealed differences of approximately 6% in the calculated surface dose, a maximum deviation of 10% at one calculation point in a high gradient region, and deviations of 3% or less for depths greater than 1.5 cm. We referred back to our original data interpolation from the small depth dose graphs which had been plotted on semi-logarithmic scale, magnified these graphs to full-page size and repeated the data interpolation from the larger graphs. Based on this information, we located interpolation differences of up to approximately 6%. The revised depth dose data set was entered into the standard treatment planning program data base and the calculations were repeated. Using the revised data set, the deviation remained 6% on the surface (.501 compared to .532), with a maximum difference of 7.5% (.151 compared to .163) at a depth of 0.5 cm. Between depth of 1.0 cm and isocenter depth of 5 cm, agreement is improved to within 2%. Using depth dose data for the Simulated Proton Event 10 July 1959, plane-wave calculations of surface dose for cylindrical phantom diameters ranging from 10 cm to 20 cm showed predicted surface dose varying from 52% to 53% of the incident flux. The 2-D rotation calculation on the phantom skull predicted a surface dose of 46.1% of the incident flux. This calculation suggests that the isodose distributions displayed in this report may underestimate the maximum surface dose by as much as 10% (.461 compared to .52), while relative doses at depths below the phantom surface will be estimated to within 3%. This result may reflect a potential limitation of applying the isodose calculation techniques, which interpolate between dose grid points, to determination of dose in a high gradient region. For the Simulated Proton Event 10 July 1959, a positional shift of 1 mm introduces a 16% change in depth dose. Additional work is needed to evaluate this difference in surface dose predictions with calculation technique.

RESULTS

Calculated isodose distributions in the transverse plane intersecting isocenter are included in Figures 1-15 for each of the 3 solar flare events for fixed field irradiation, 2-D rotation, and 3-D rotation. For the 2-D rotation, doses are also reported in the most superior plane, corresponding to the crown of the head. Additionally, isodose distributions are recorded in the sagittal plane intersecting isocenter for the 3-D rotation. In all cases, the isodoses are reported relative to the dose at isocenter (100 centigray) in the absence of the head phantom. Wire-frame models of the head phantom indicating the calculation plane and the rotation plane for

each arc segment in the 3-D rotation are included in pages 22-36. A comparison of dose at isocenter vs. dose at the phantom surface is presented for each solar flare event in Table 1.

EVALUATION OF RESULTS

The isodose calculations for the 3 solar particle events reviewed show that, in all calculation configurations, the maximum predicted dose will be on the exterior surface of the head phantom. The relative surface dose to the phantom increases with increasing energy of the solar flare event; this is attributed to the greater exit dose achieved due to increased penetrability of the solar particles with the increasing energy. The minimum dose within the phantom increases with the energy of the solar event. For a given solar event, the minimum dose within the head phantom is approximately the same for both 2-D and 3-D rotation calculations, indicating that the average depth to that calculation point remains approximately the same for both calculations. This depth is realistic for the head; however we would expect to see a greater difference between 2-D and 3-D rotation calculations if applied to the thorax, abdomen, arms or legs due to the elongated shape compared to the head. This calculational technique can equally well be applied to predictive display of dose distributions throughout the thorax and abdomen and can be used to demonstrate the effect of tissue inhomogeneities such as lungs and bones on the resultant doses received during solar events. We suggest that this be investigated in a follow-on study using these solar flare data as well as other representative examples.

These calculations suggest that the superficially located organs are at greatest risk to radiation similar to the 3 cases studied here. Thus, the lens of the eye and the skin would receive the greatest exposure. Because of the greater sensitivity of the lens, it will be the limiting organ in determining necessary shielding and exposure time limits.

TABLE 1. SIMULATED PROTON EVENT 10 JULY 1959
(CASE 1)

	<u>Dose at Isocenter</u>	<u>Dose at Surface</u>	<u>Ratio</u>
Fixed Field	1.0	101.3	
2-D Rotation	0.8	46.1	0.017
(superior plane)	3.55	47.1	0.075
3-D Rotation	0.75	27.8	0.027

SIMULATED PROTON EVENT 23 FEBRUARY 1956
(CASE 2)

	<u>Dose at Isocenter</u>	<u>Dose at Surface</u>	<u>Ratio</u>
Fixed Field	6.	101.4	
2-D Rotation	5.1	50.3	0.101
(superior plane)	12.0	54.0	0.222
3-D Rotation	4.9	38.0	0.128

SIMULATED PROTON EVENT 16 FEBRUARY 1984
(CASE 3)

	<u>Dose at Isocenter</u>	<u>Dose at Surface</u>	<u>Ratio</u>
Fixed Field	13.	103.5	
2-D Rotation	11.1	57.8	0.192
(superior plane)	23.9	63.1	0.379
3-D Rotation	10.6	55.6	0.191

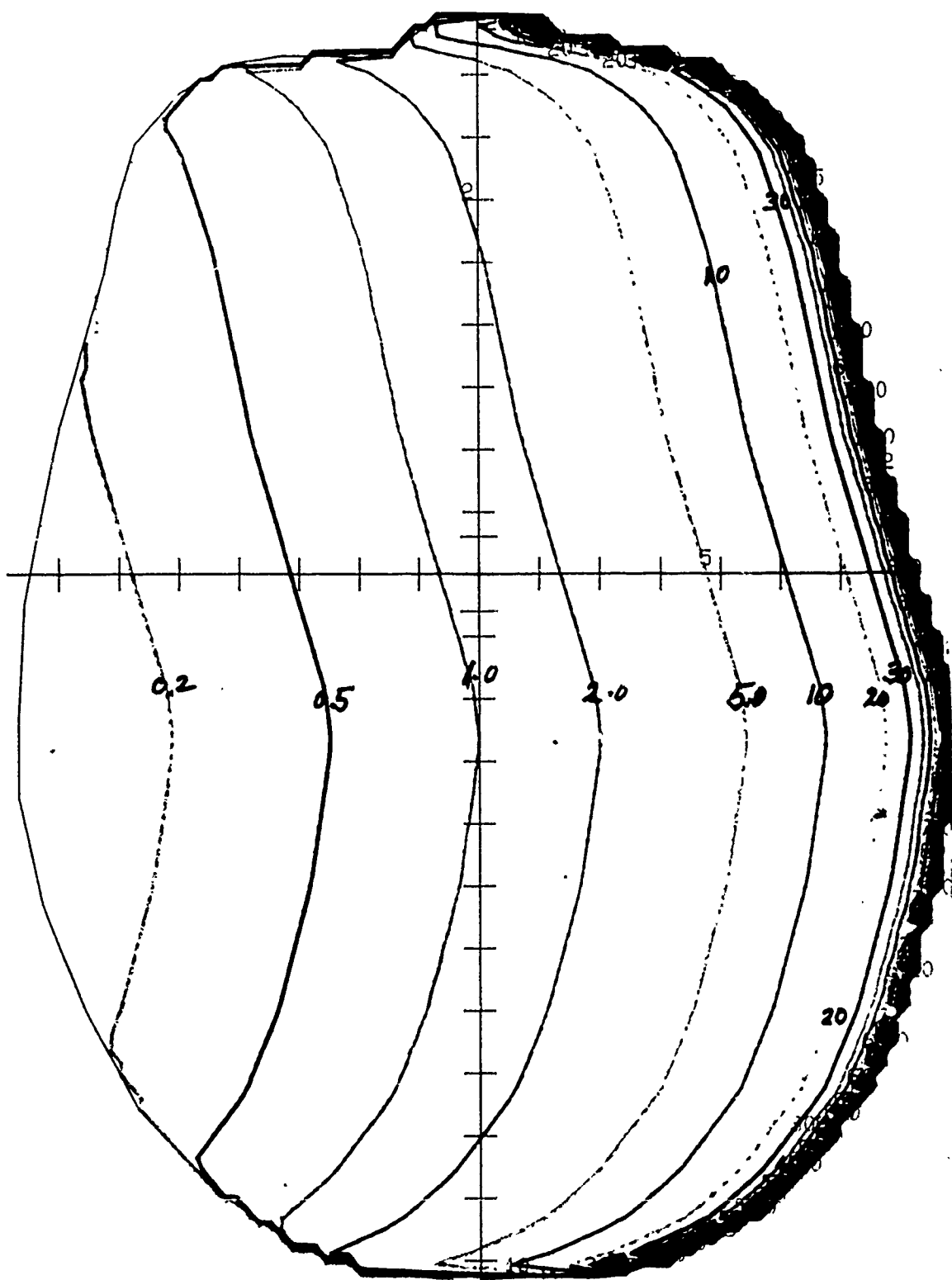


Figure 1. Simulated proton event 10 July 1959. Fixed field isodose distribution (isocenter transverse plane).

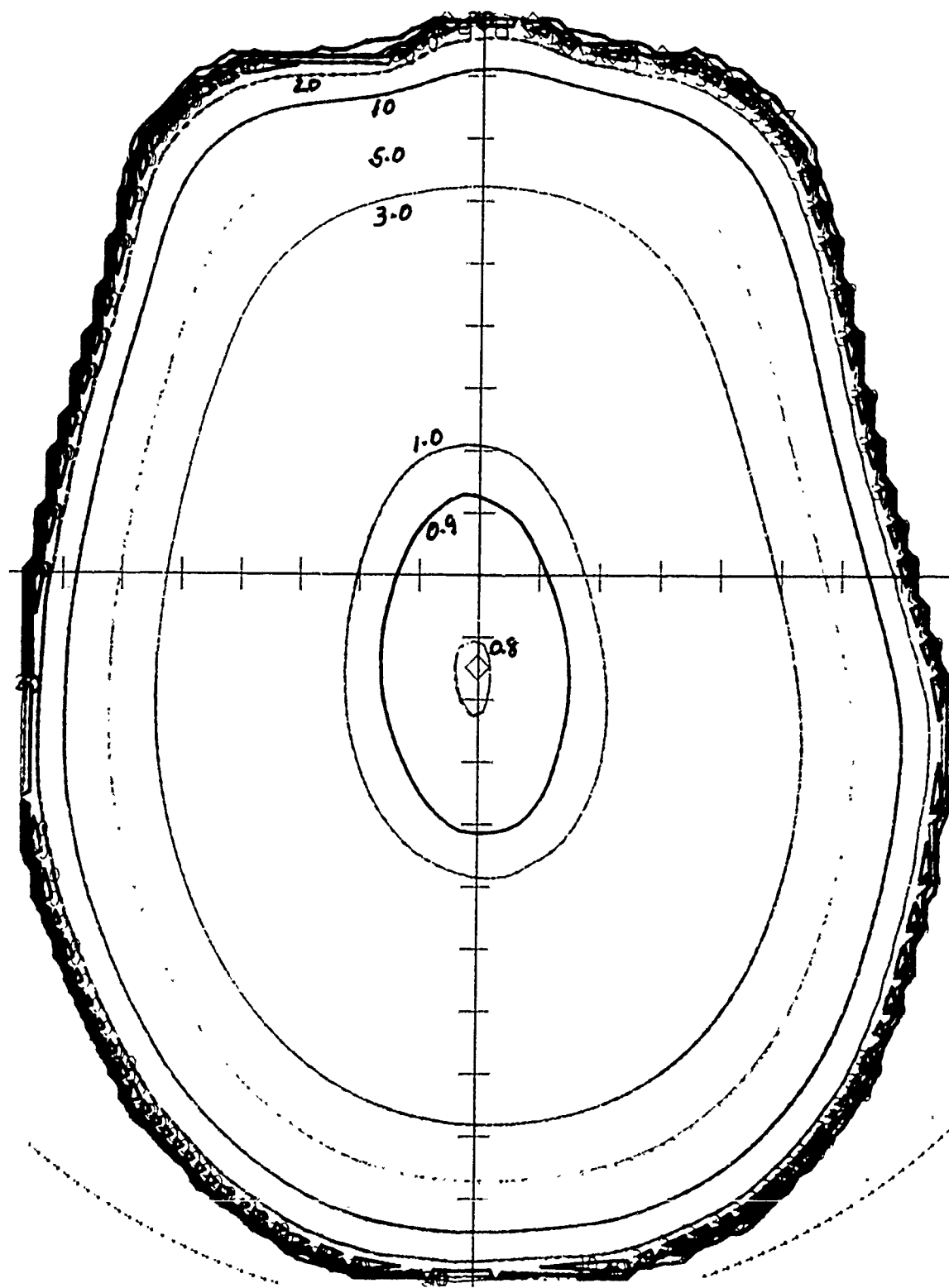


Figure 2. Simulated proton event 10 July 1959. Two-dimensional rotation isodose distribution (isocenter transverse plane).

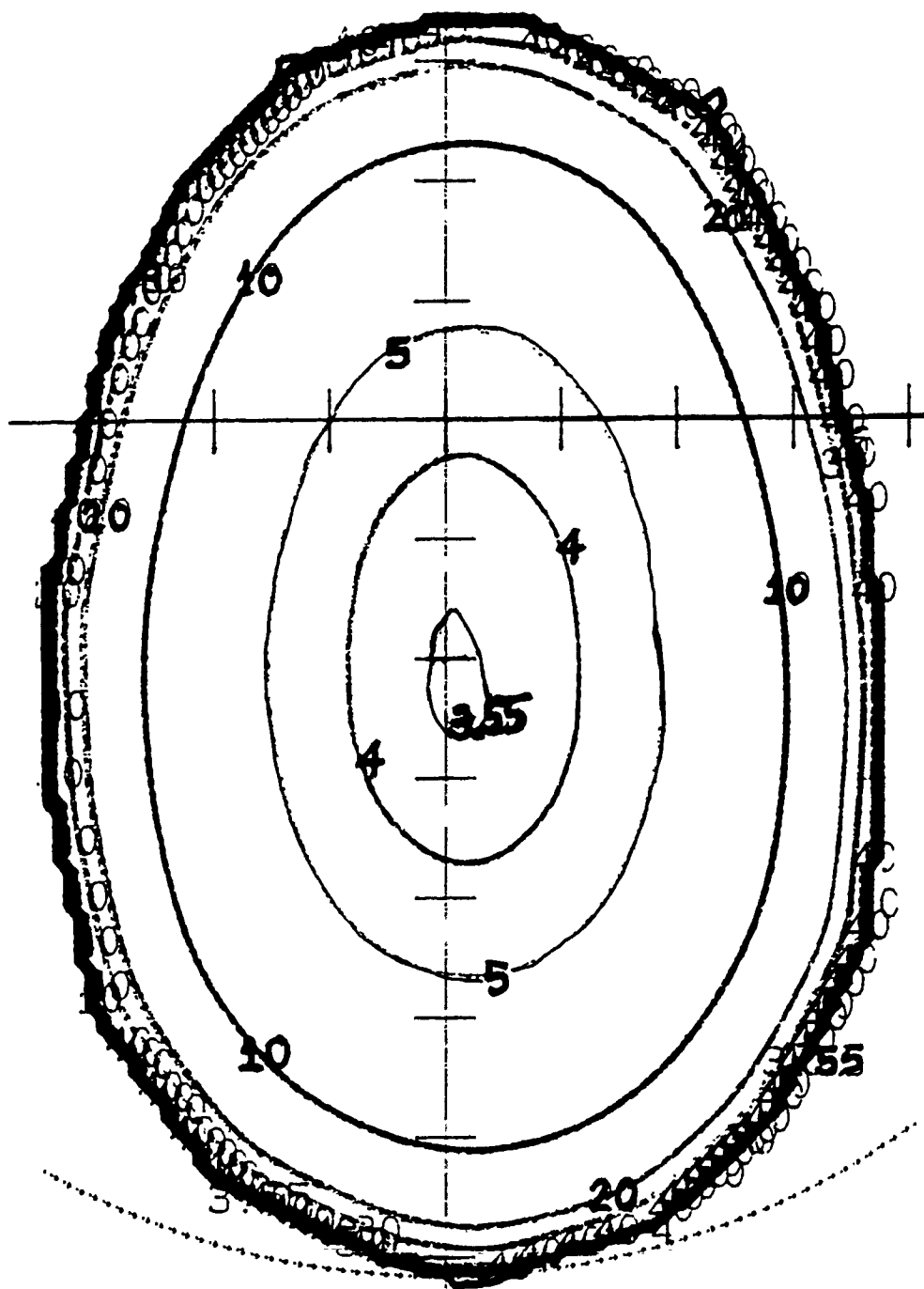


Figure 3. Simulated proton event 10 July 1959. Two-dimensional rotation isodose distribution (superior transverse plane).

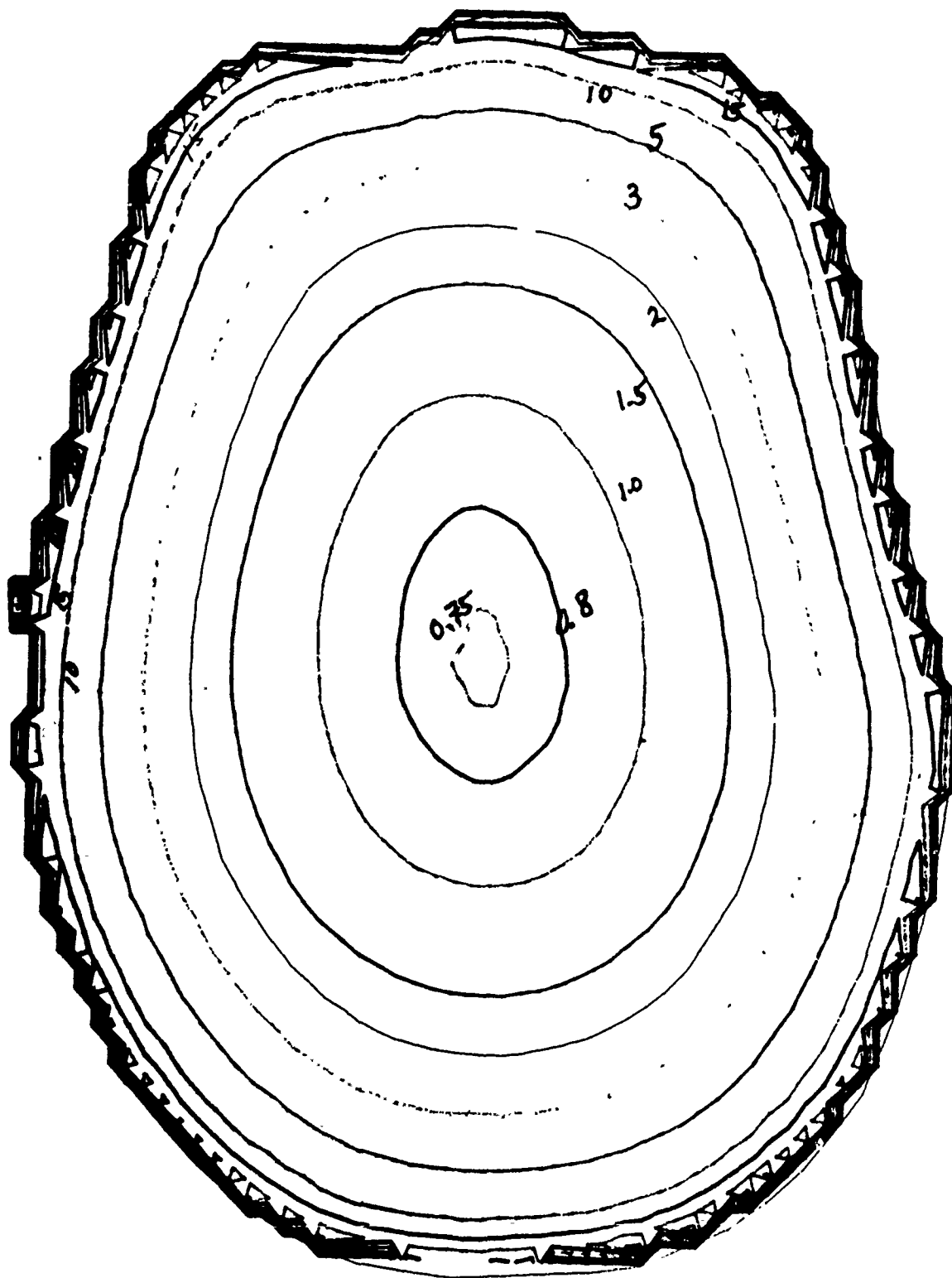


Figure 4. Simulated proton event 10 July 1959. Three-dimensional rotation isodose distribution (isocenter transverse plane).

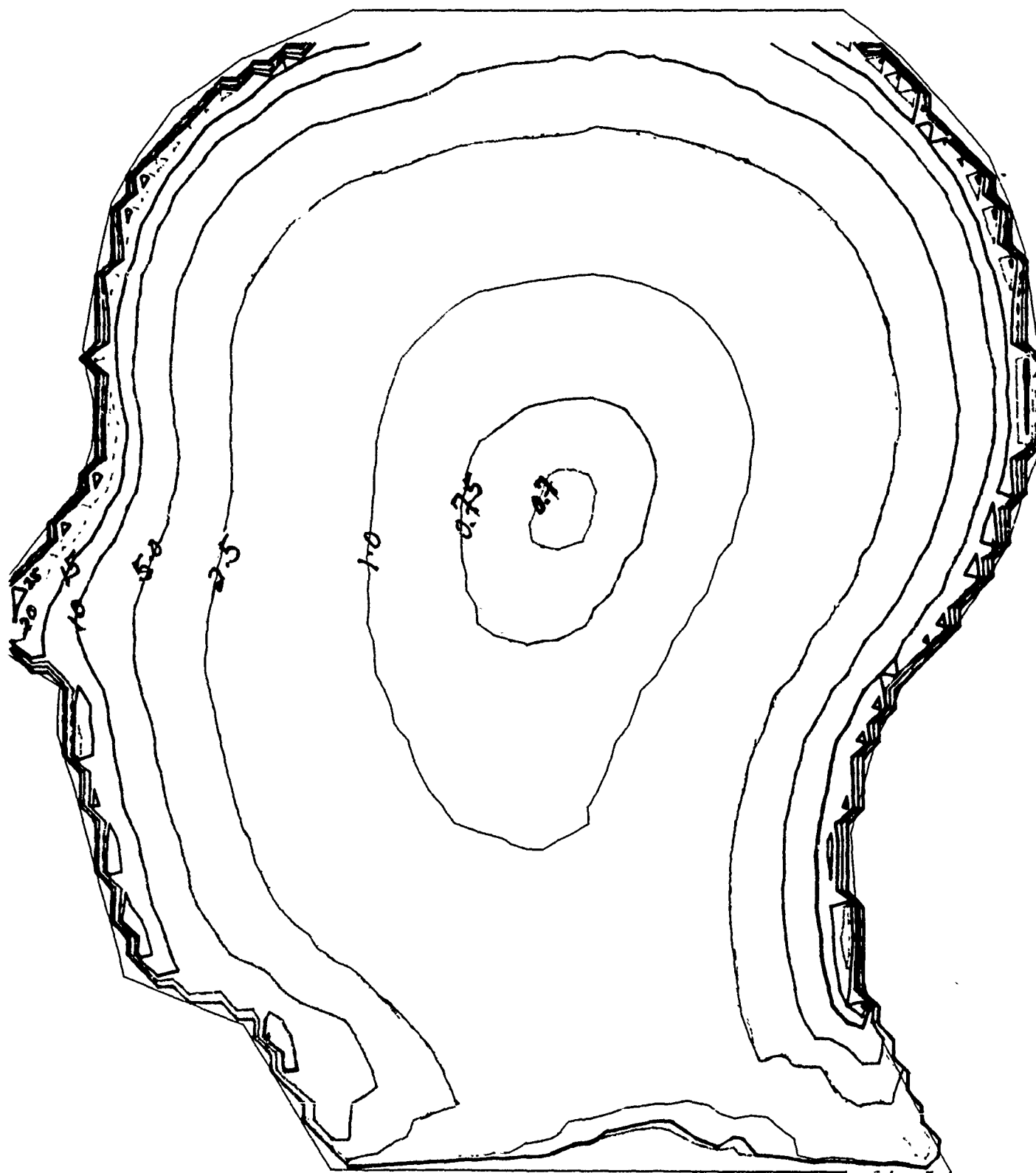


Figure 5. Simulated proton event 10 July 1959. Three-dimensional rotation isodose distribution (isocenter sagittal plane).

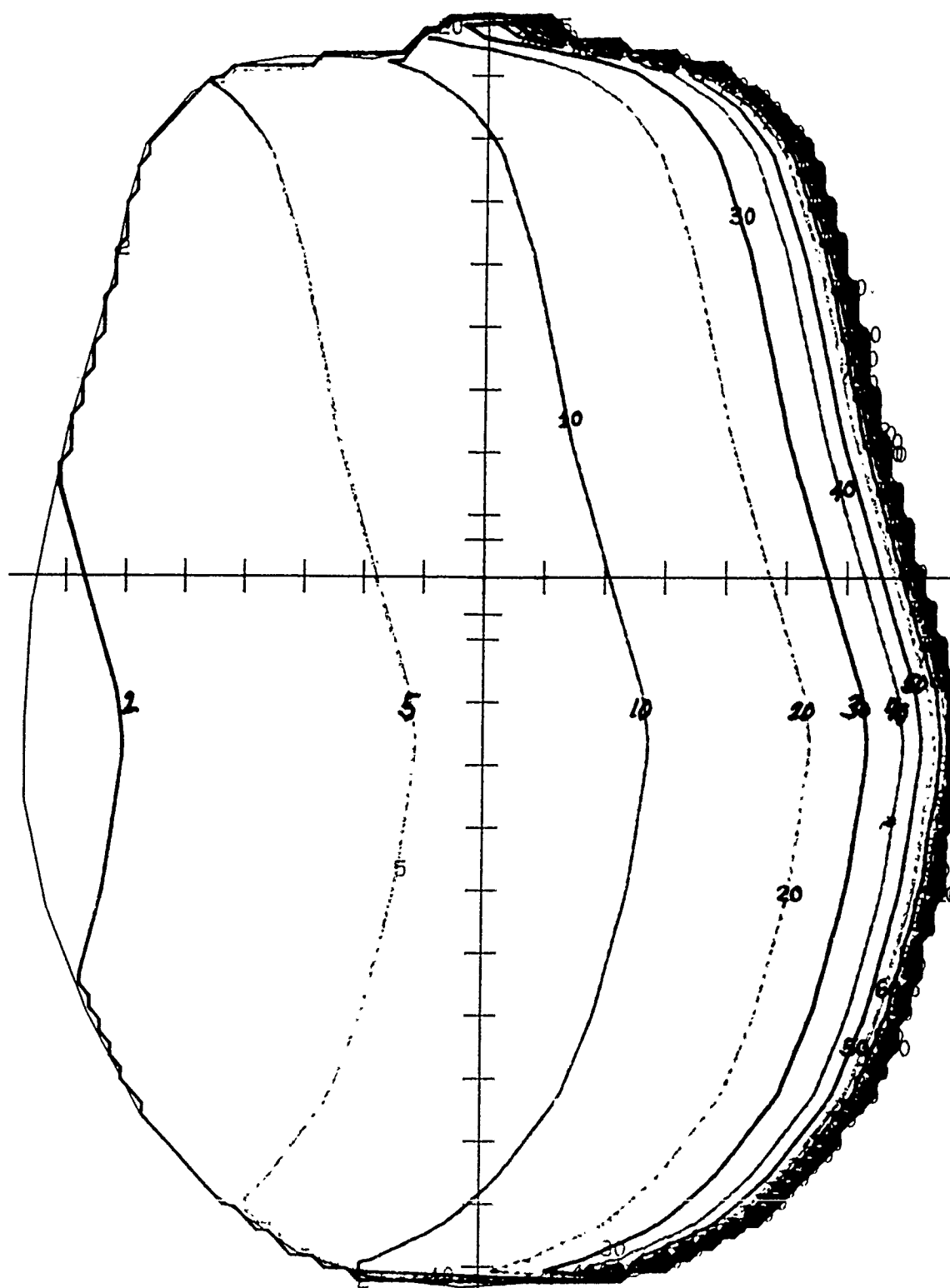


Figure 6. Simulated proton event 23 February 1956. Fixed field isodose distribution (isocenter transverse plane).

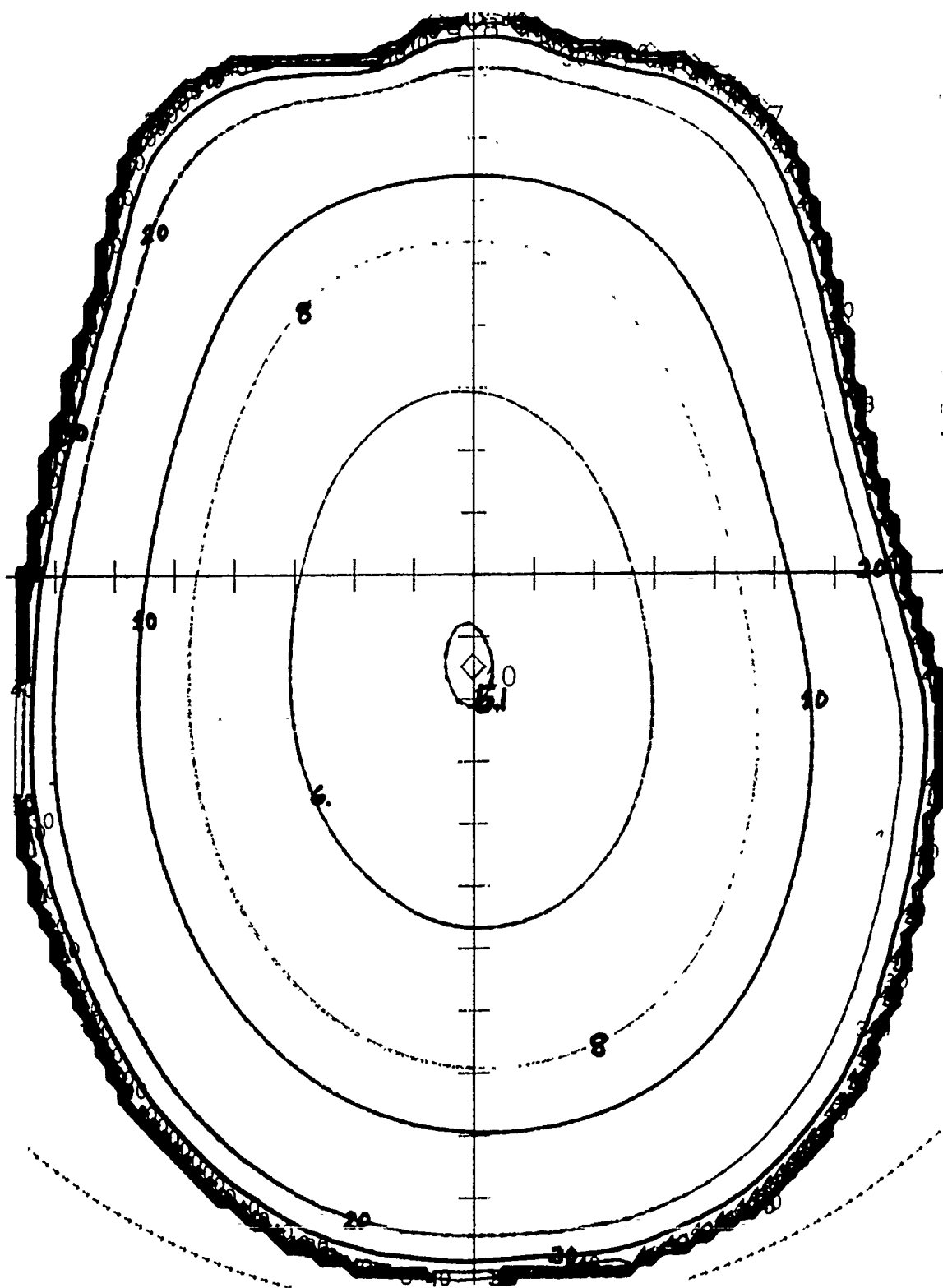


Figure 7. Simulated proton event 23 February 1956. Two-dimensional rotation isodose distribution (isocenter transverse plane).

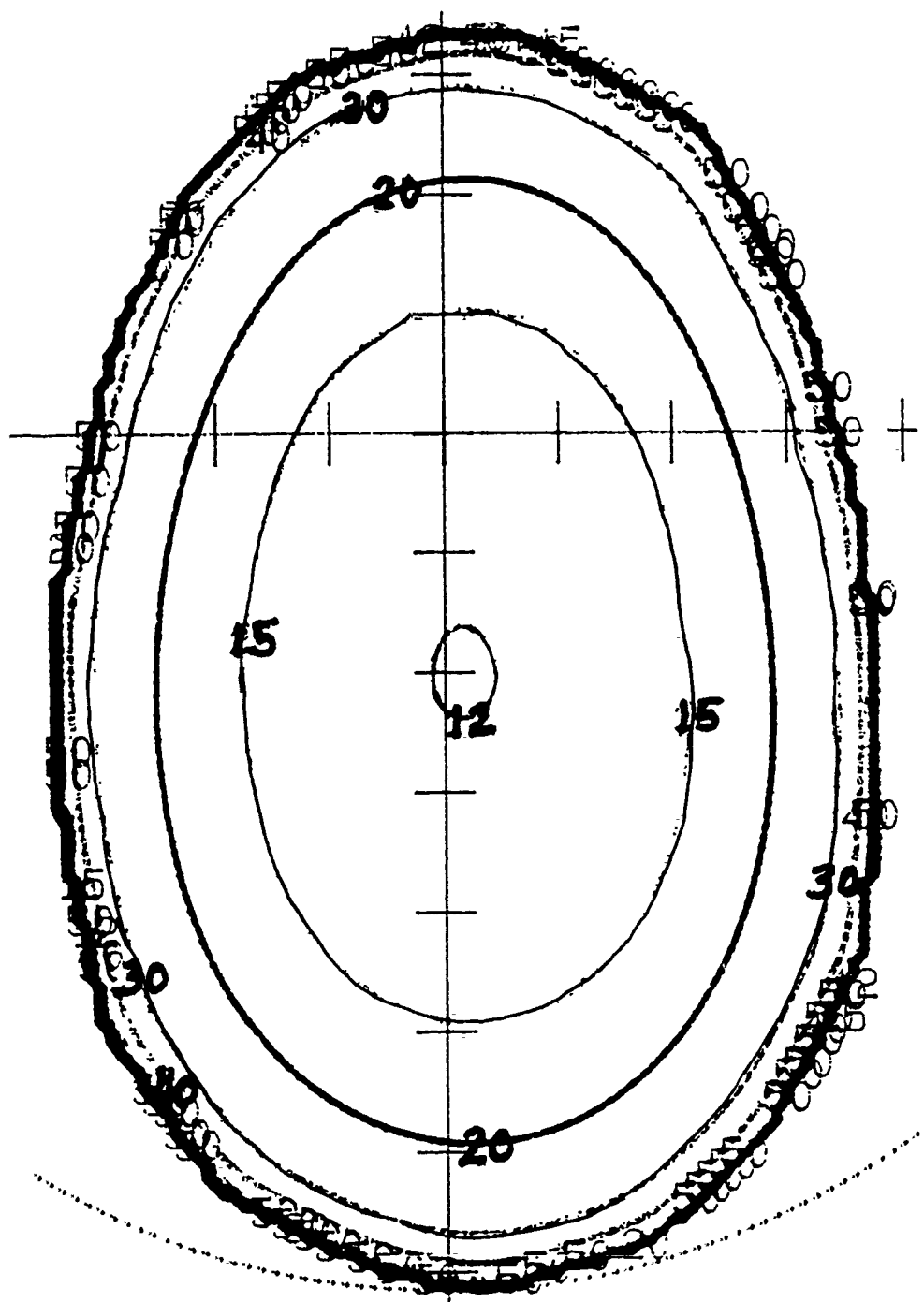


Figure 8. Simulated proton event 23 February 1956. Two-dimensional rotation isodose distribution (superior transverse plane).

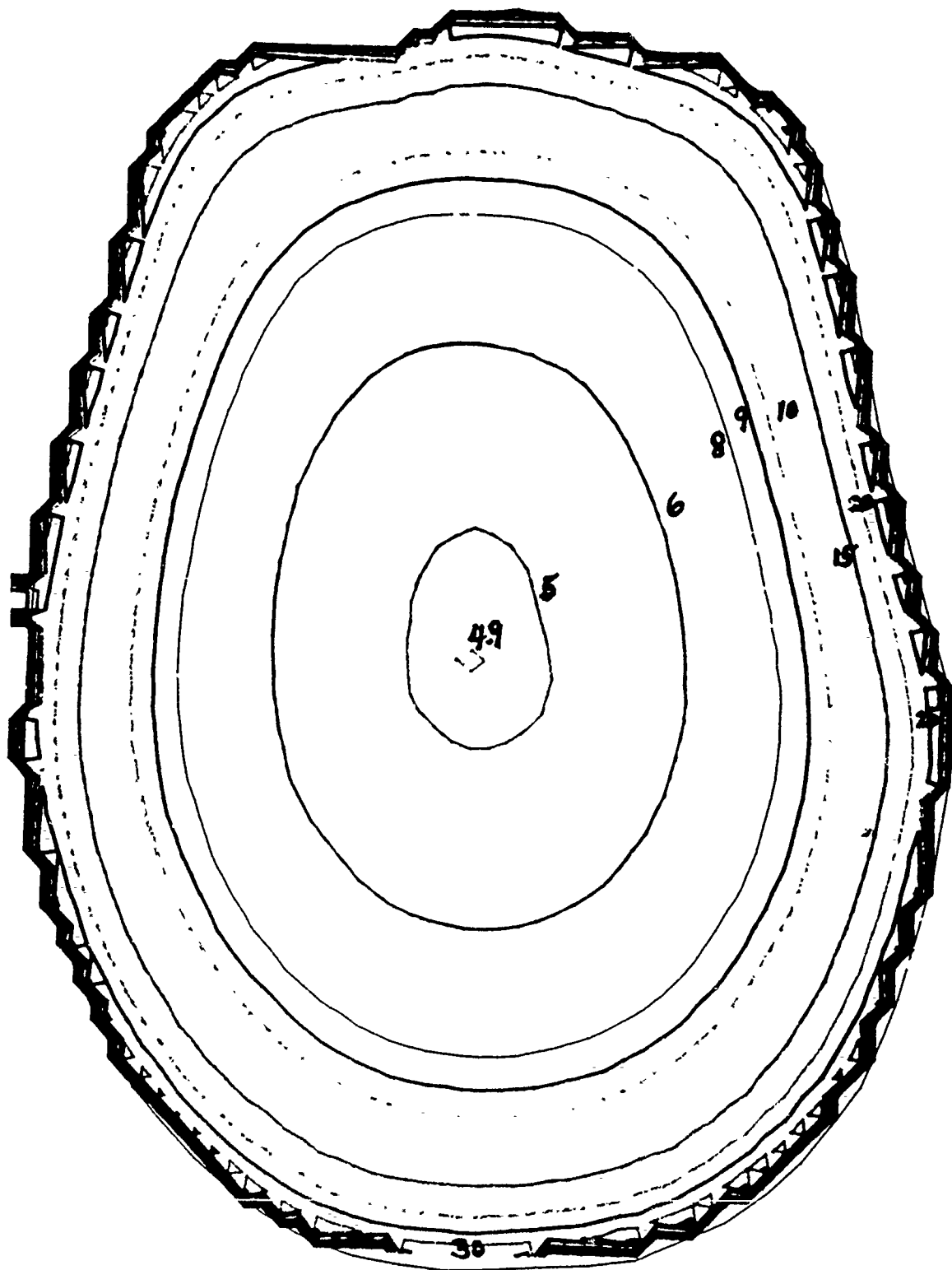


Figure 9. Simulated proton event 23 February 1956. Three-dimensional rotation isodose distribution (isocenter transverse plane).

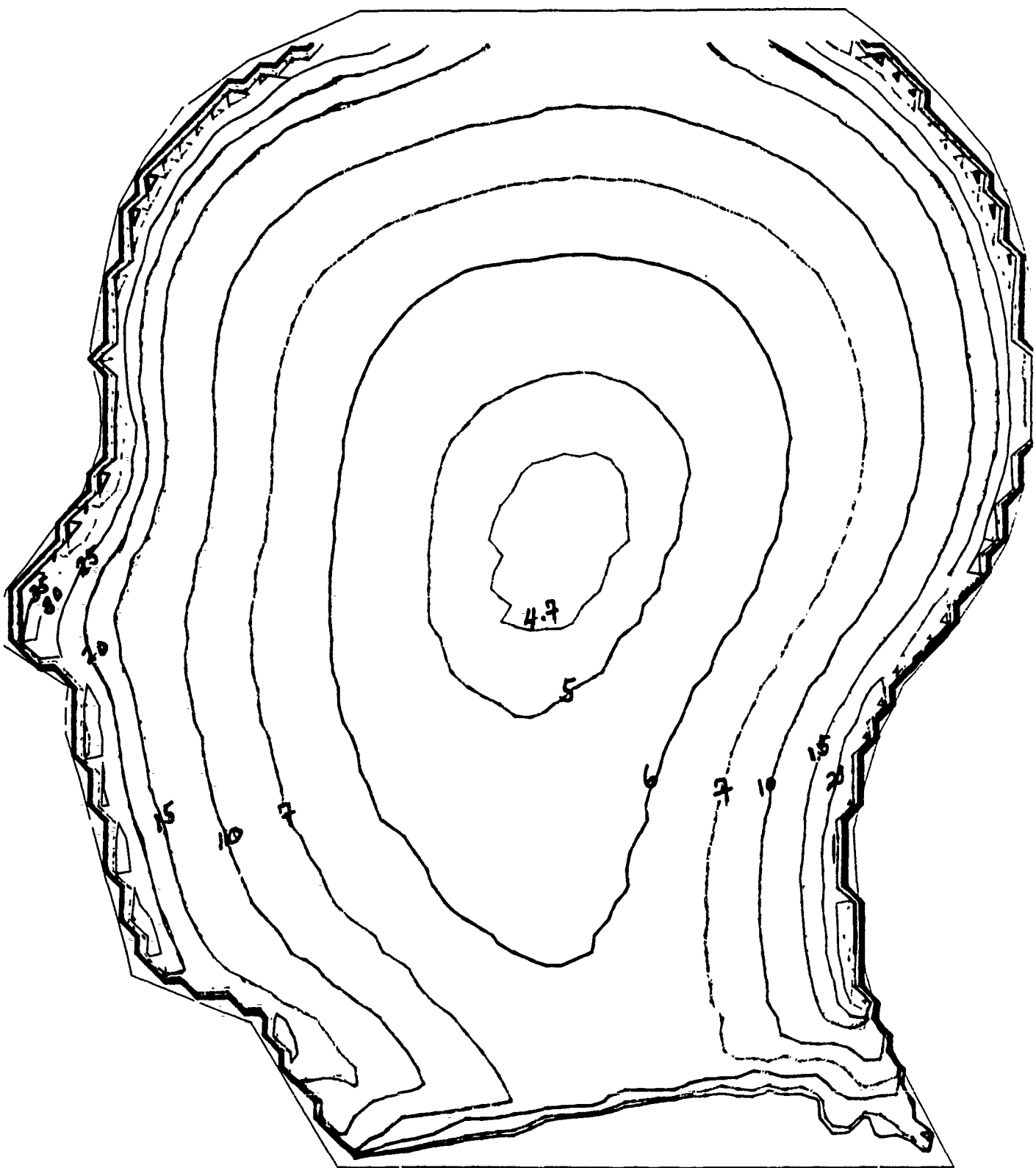


Figure 10. Simulated proton event 23 February 1956. Three-dimensional rotation isodose distribution (isocenter sagittal plane).

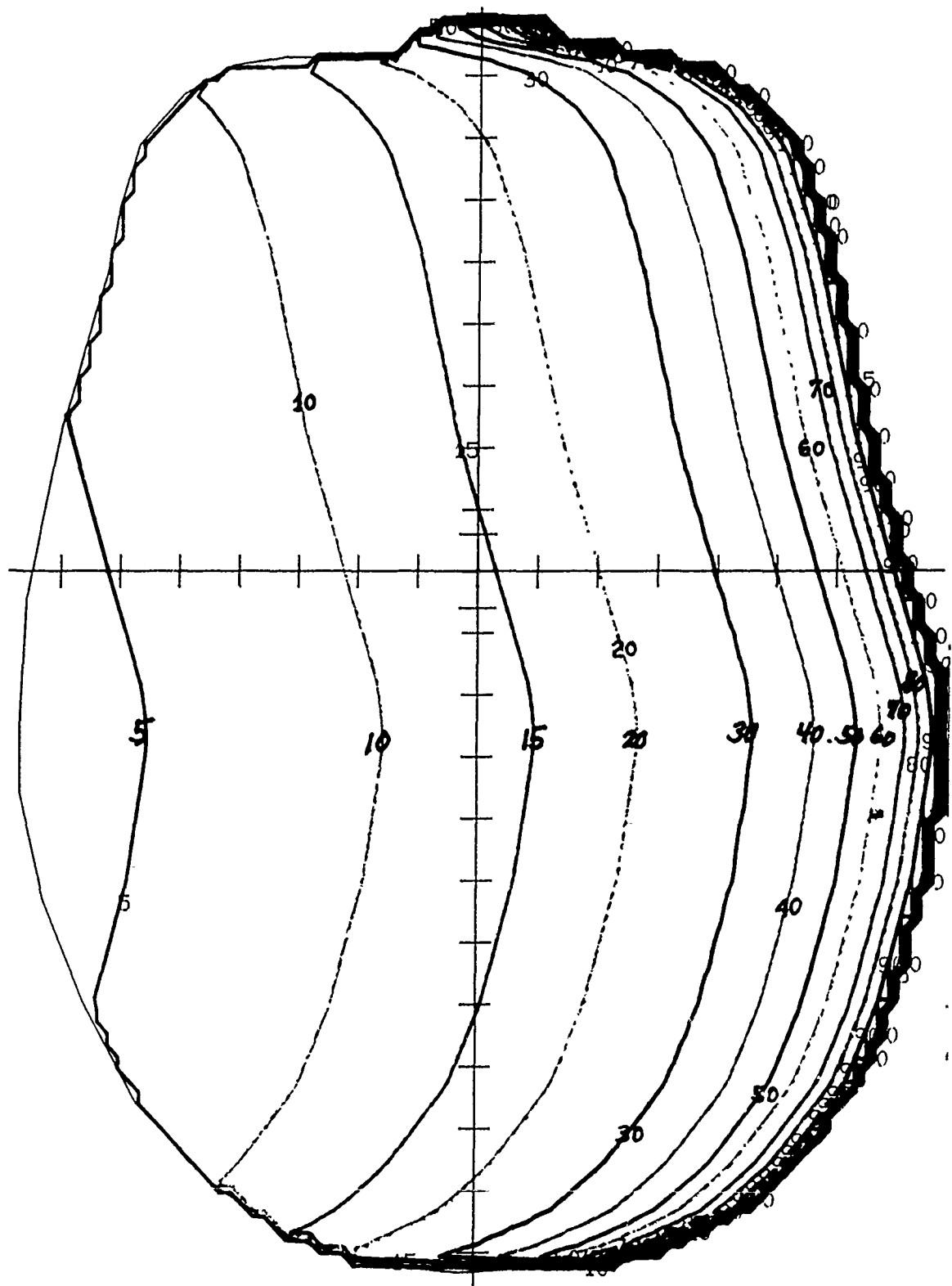


Figure 11. Solar particle event 16 February 1984. Fixed field isodose distribution (isocenter transverse plane).

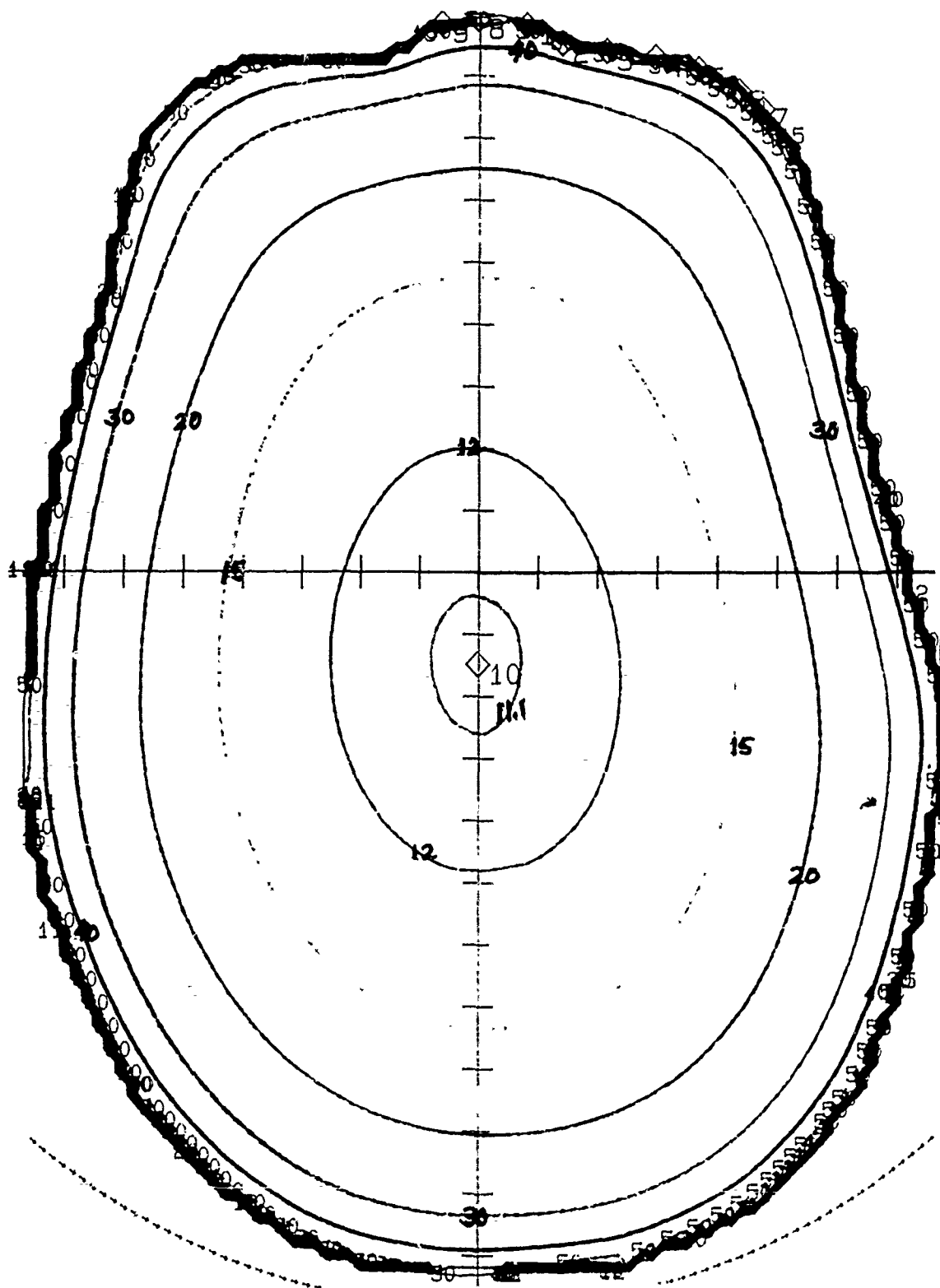


Figure 12. Solar particle event 16 February 1984. Two-dimensional rotation isodose distribution (isocenter transverse plane).

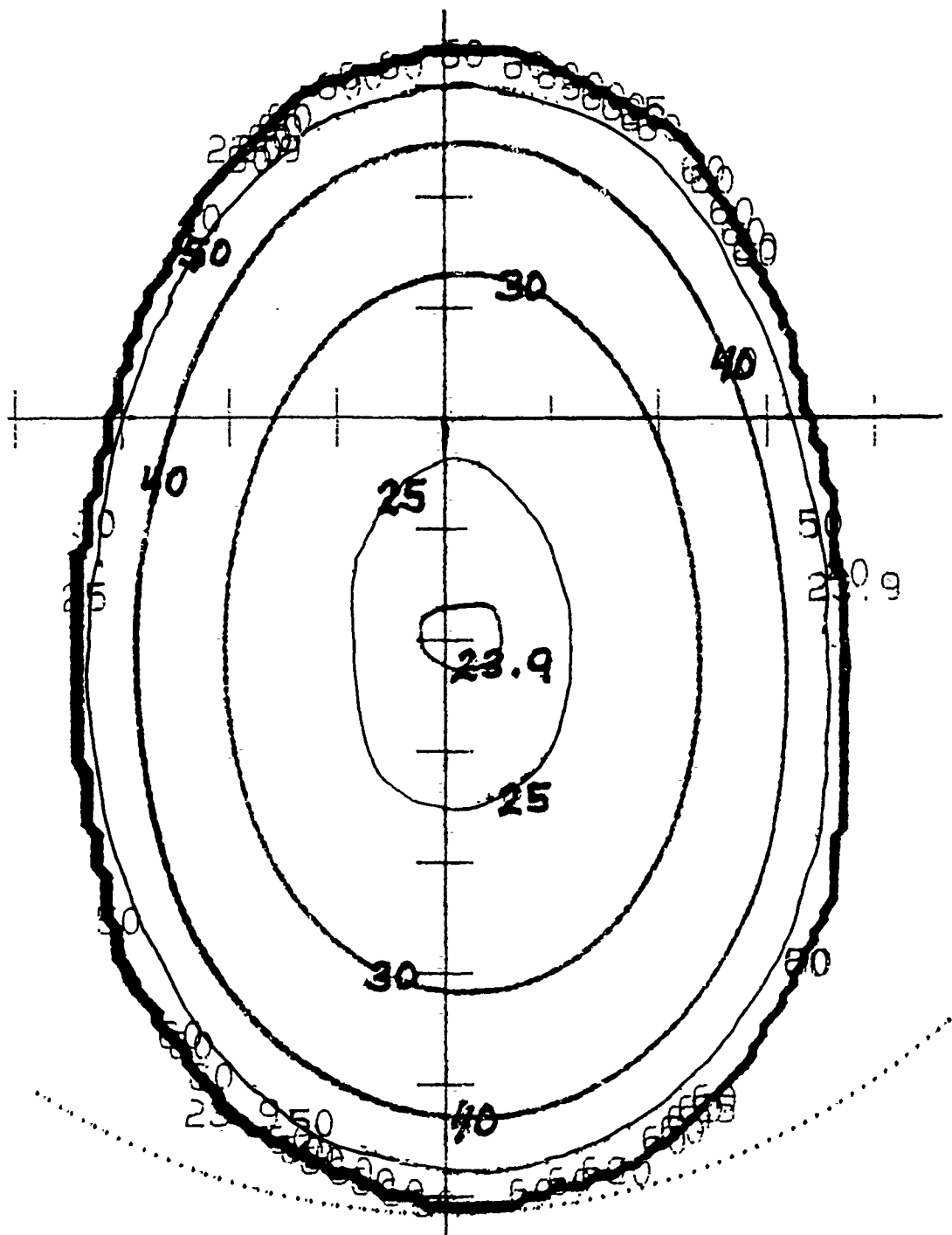


Figure 13. Solar particle event 16 February 1984. Two-dimensional rotation isodose distribution (superior transverse plane).

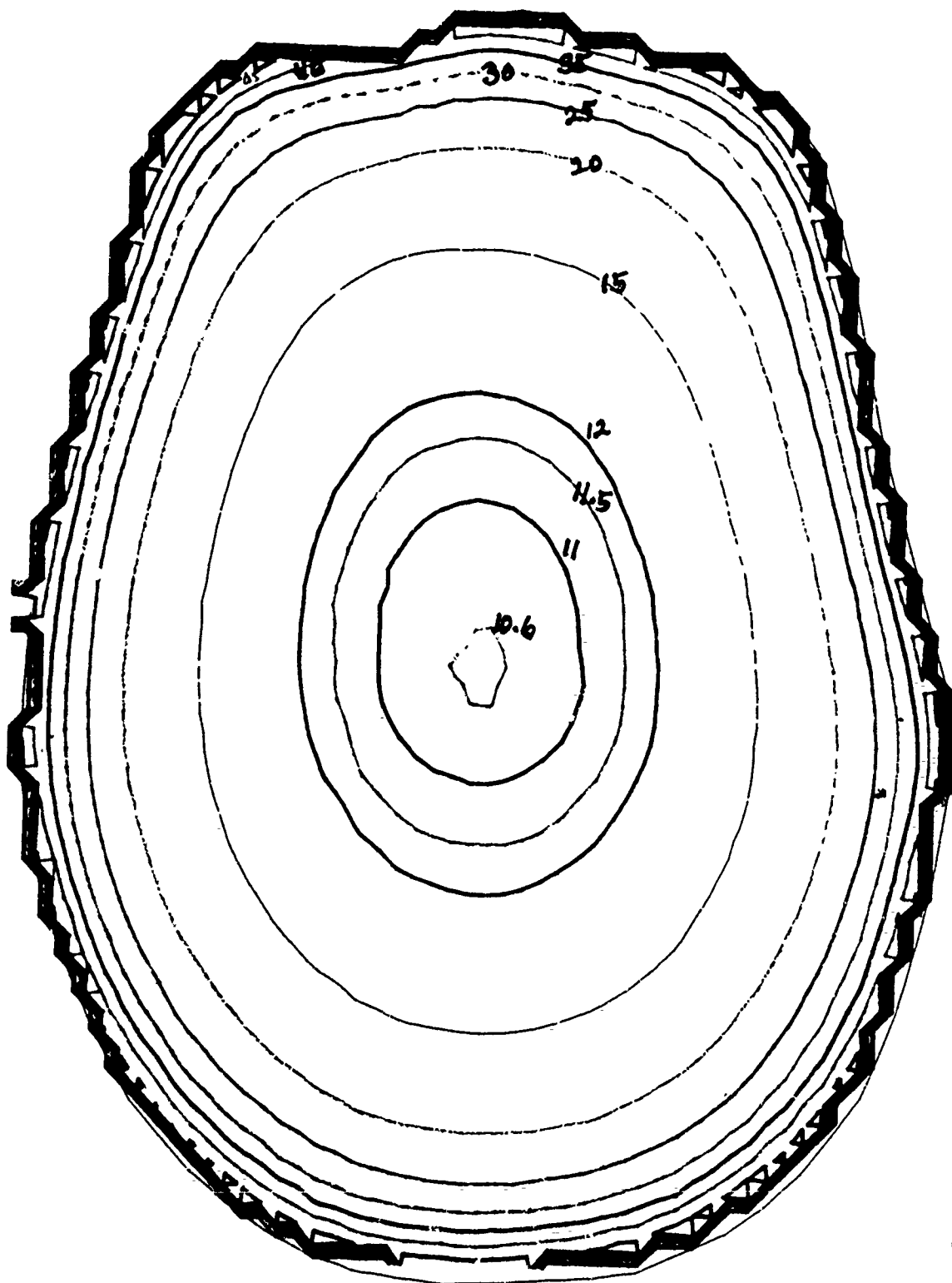


Figure 14. Solar particle event 16 February 1984. Three-dimensional rotation isodose distribution (isocenter transverse plane).

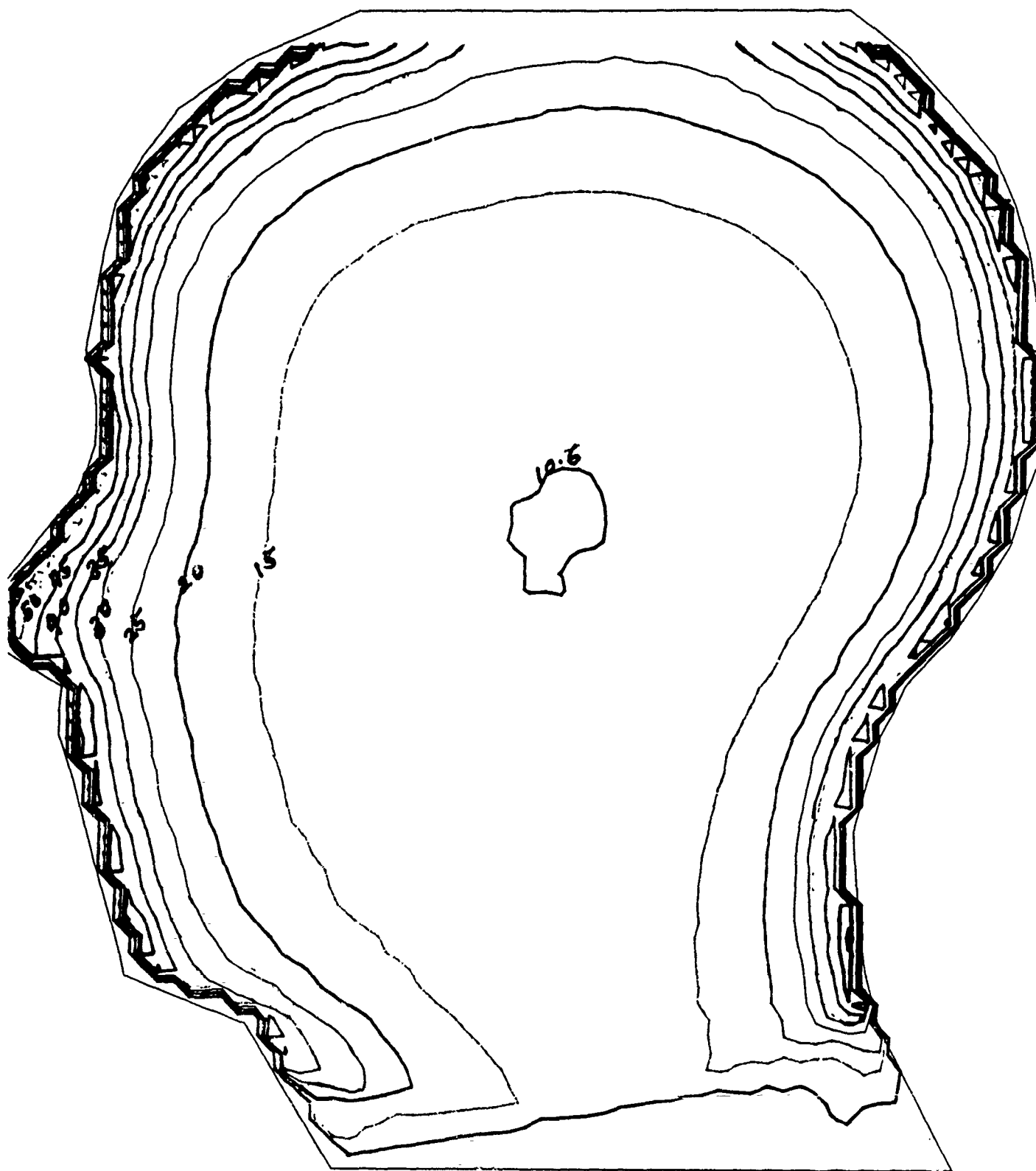


Figure 15. Solar particle event 16 February 1984. Three-dimensional rotation isodose distribution (isocenter sagittal plane).

The following wire-frame graphics displays illustrate the 3-D orientation of the head phantom during the sequence of arc rotation calculations.

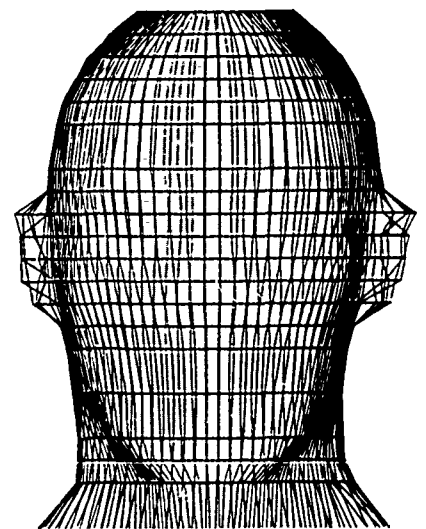
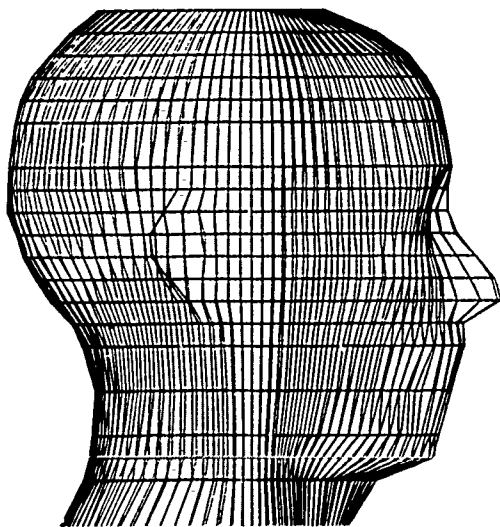
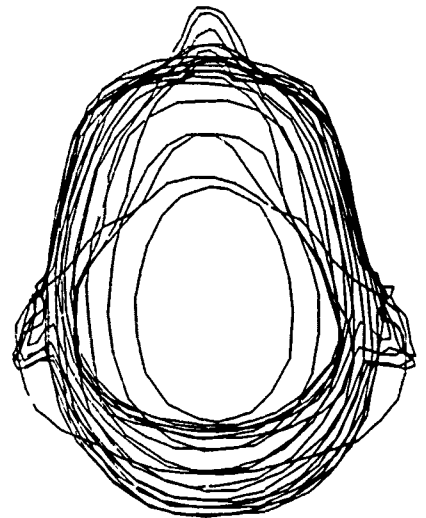
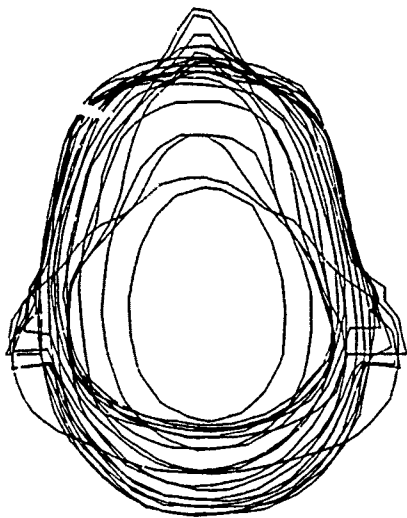
- p.22 3-D reconstruction of the head phantom from the computerized tomography scans. The top two views demonstrate the phantom contour outline in each of 20 CT slices. The bottom two views show the wire-frame reconstruction of the head phantom as viewed from the side and the front.

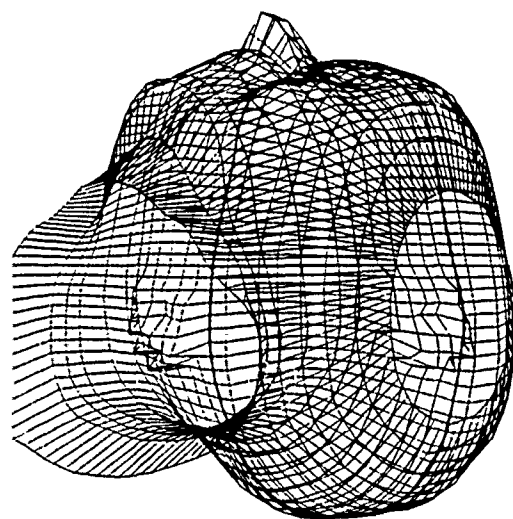
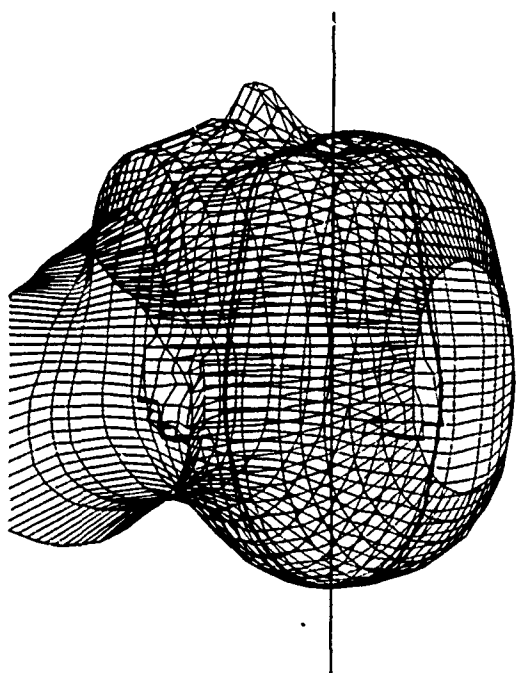
- p.23 Head positioned -40 degrees relative to normal incidence of radiation field. Upper left: Lateral view of head as rotated -40 degrees. Vertical line is plane of rotation of radiation field. Solid contour line is intersection of transverse calculation plane with head phantom. Lower left: Anterior view of head. Horizontal line is plane of rotation of radiation field. Line at 40 degrees below horizon is transverse calculation plane. Lower right: Limits of arc segment for this orientation. In all succeeding displays the same general description applies. Only the angle of the head phantom relative to the plane of radiation field rotation is changed.

- p.24 Head positioned at -20 degrees.
- p.25 Head positioned at 0 degrees. Note that the transverse calculation plane is coincident with the plane of rotation of the radiation field. This corresponds to the plane in which the 2-D calculations were performed.

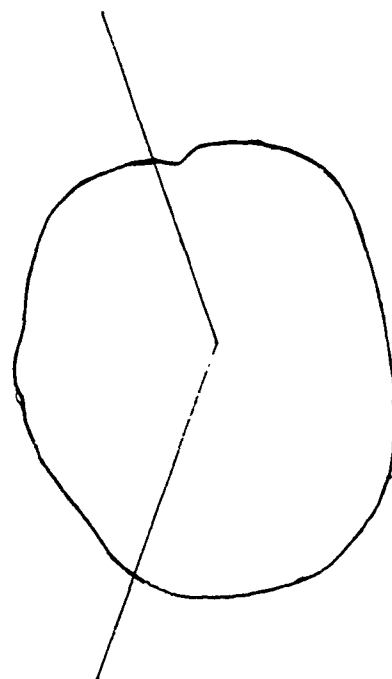
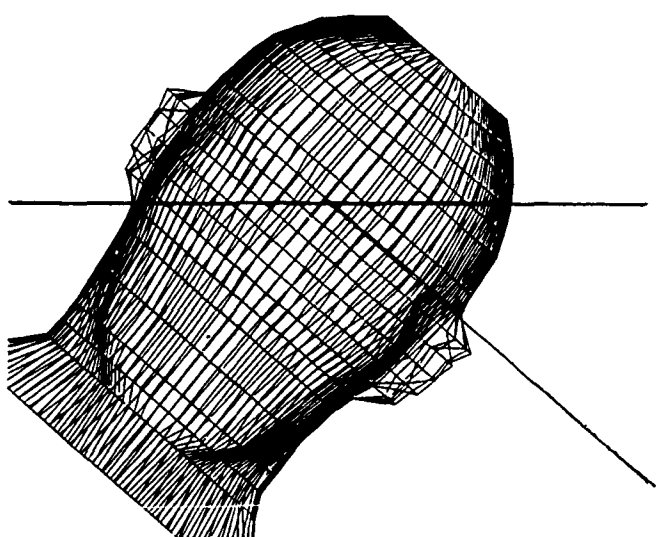
- p.26 Head positioned at 20 degrees.
- p.27 Head positioned at 40 degrees.
- p.28 Head positioned at 60 degrees.
- p.29 Head positioned at 80 degrees.
- p.30 Head positioned at 100 degrees.
- p.31 Head positioned at 120 degrees.
- p.32 Head positioned at 140 degrees.
- p.33 Head positioned at 160 degrees.
- p.34 Head positioned at 180 degrees.
- p.35 Head positioned at 200 degrees.
- p.36 Head positioned at 220 degrees.

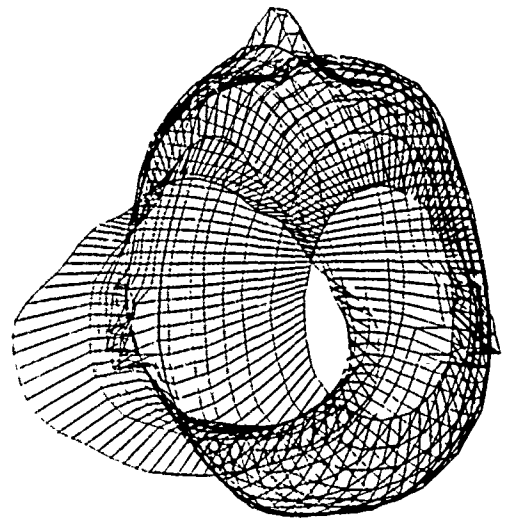
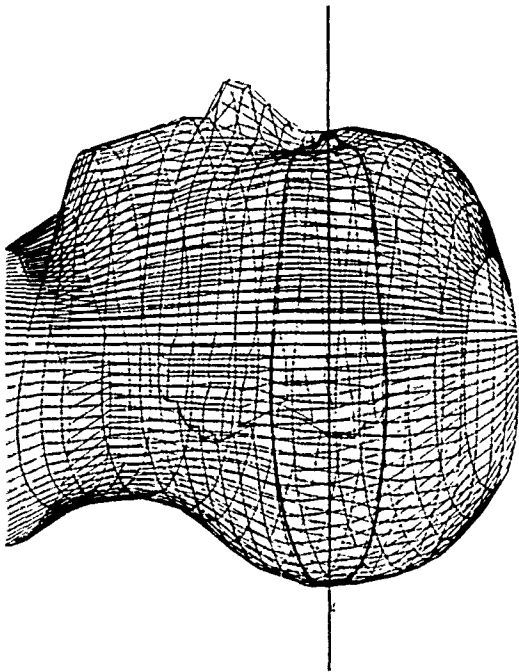
The summation of dose from the arcs represented in these views is presented as the 3-D rotation dose in the isocenter transverse plane and the isocenter sagittal plane for each of the three solar flare dose distributions.



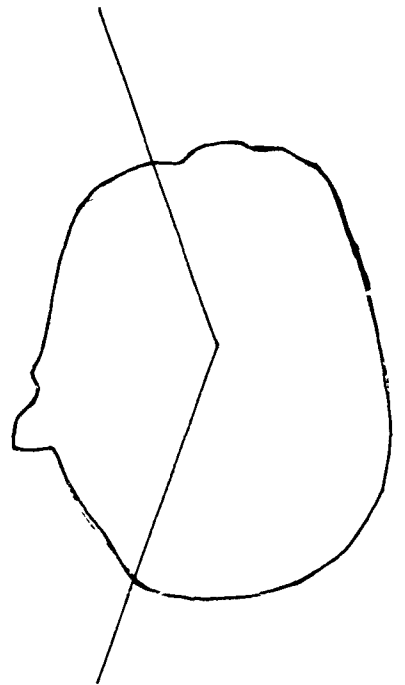
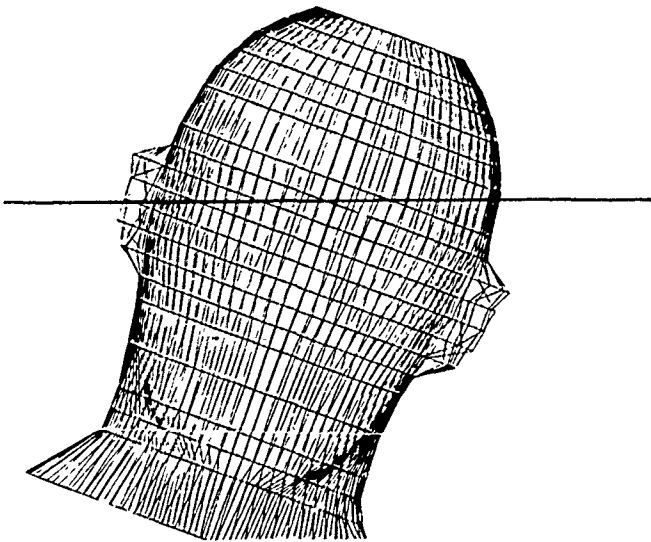


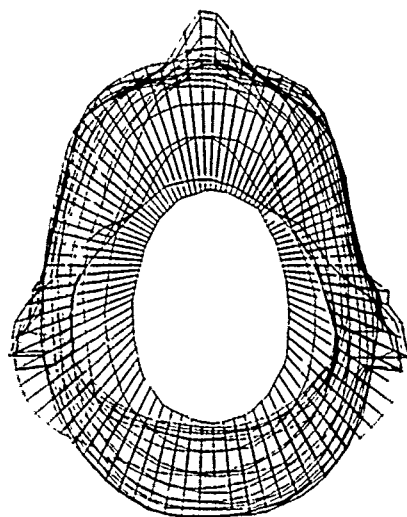
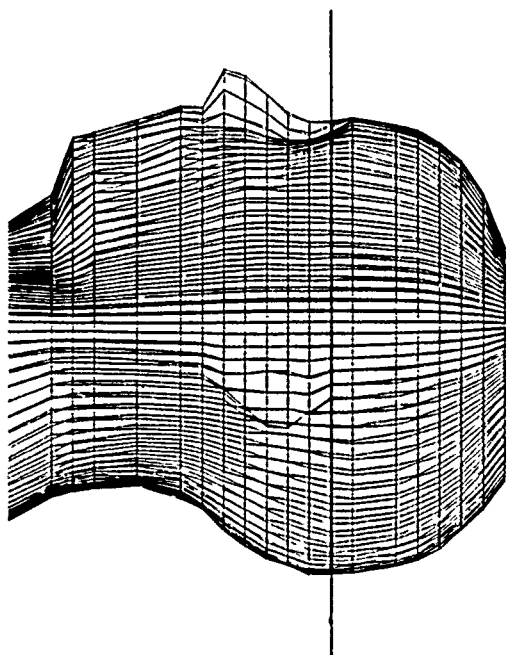
-40°



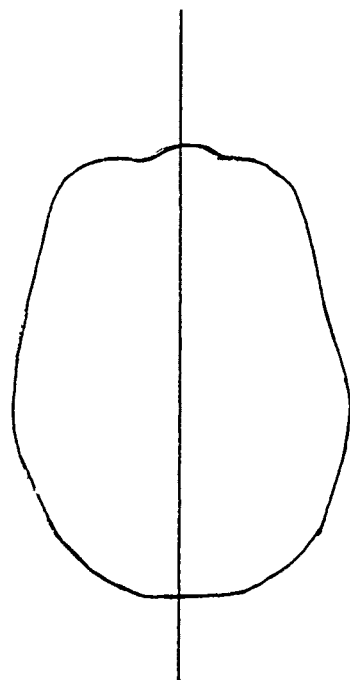
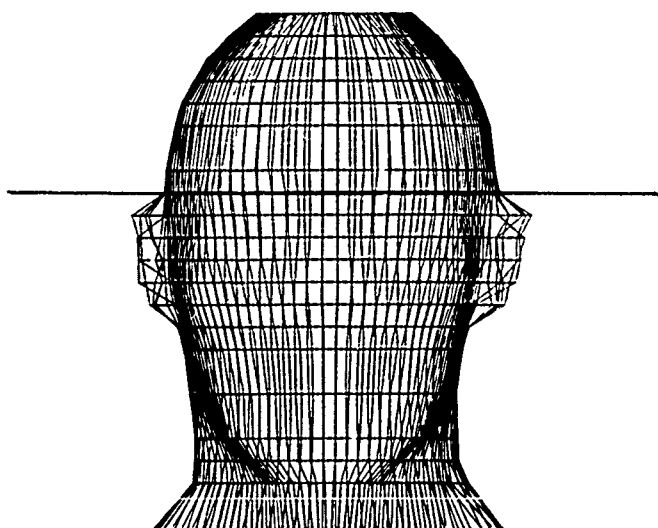


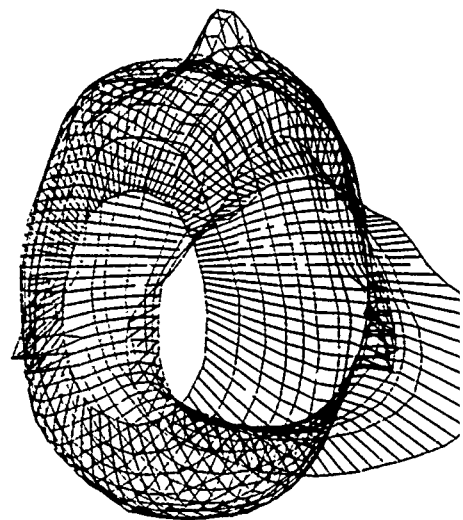
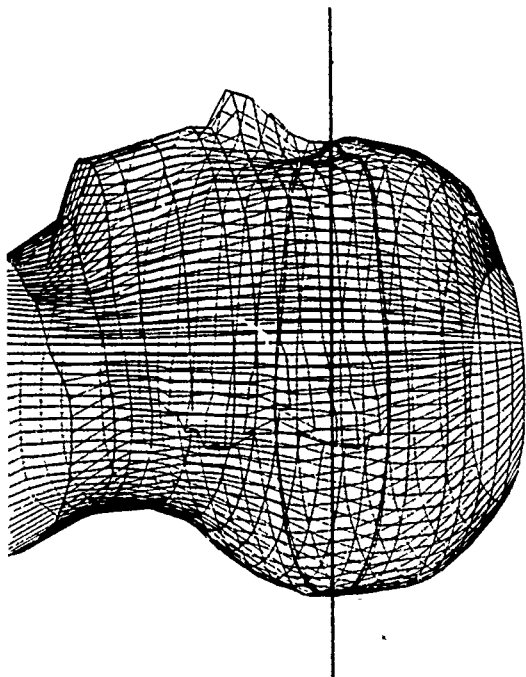
-20°



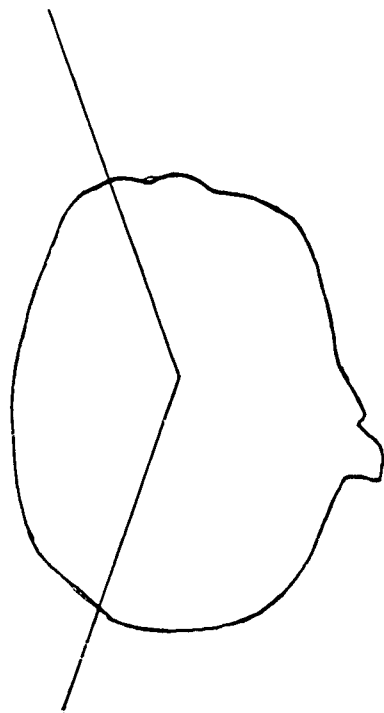
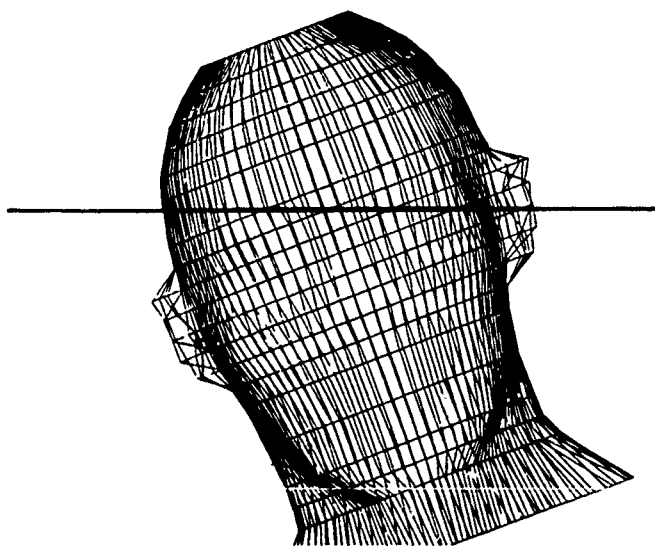


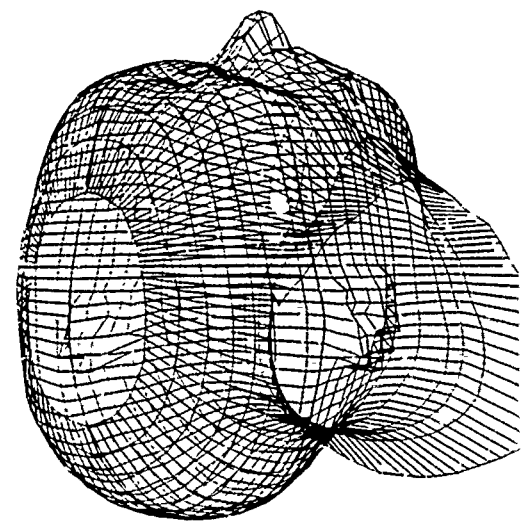
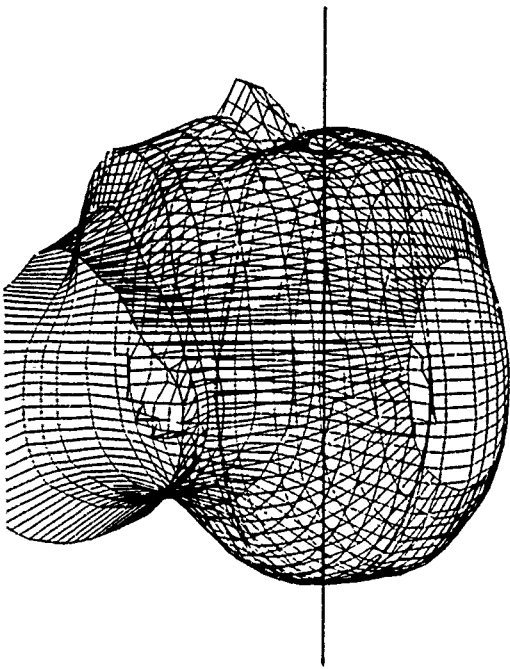
00°



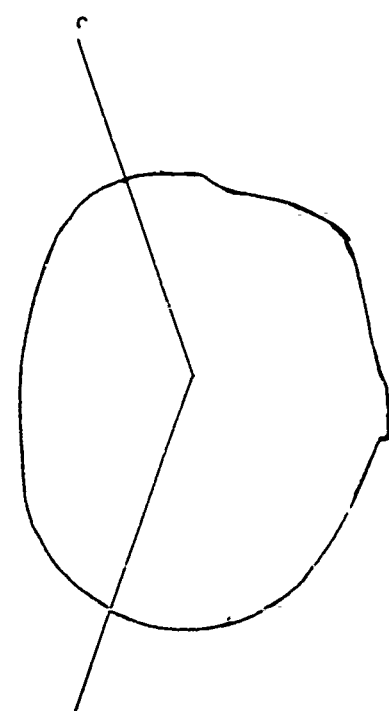
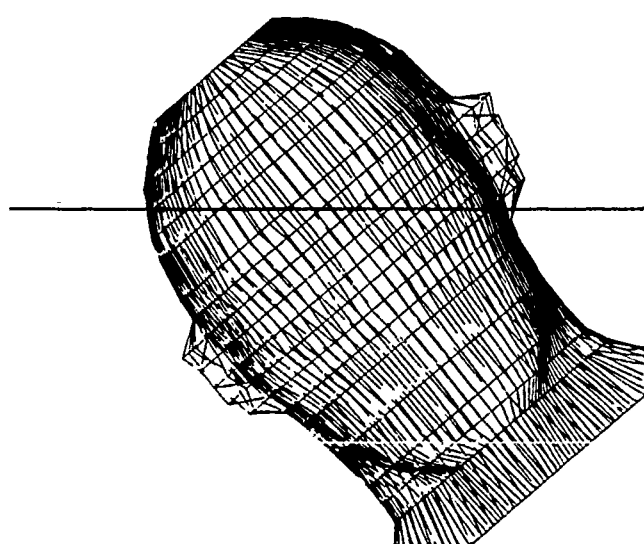


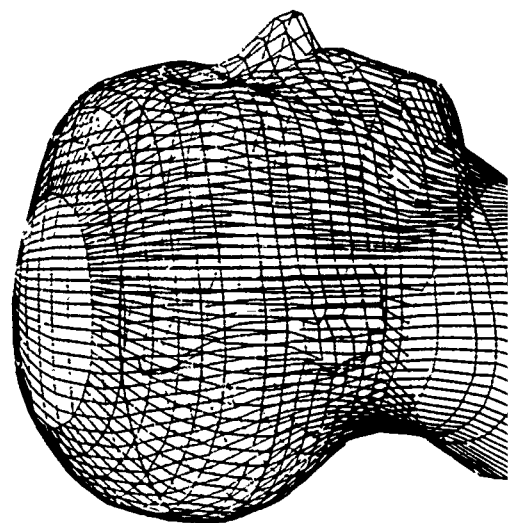
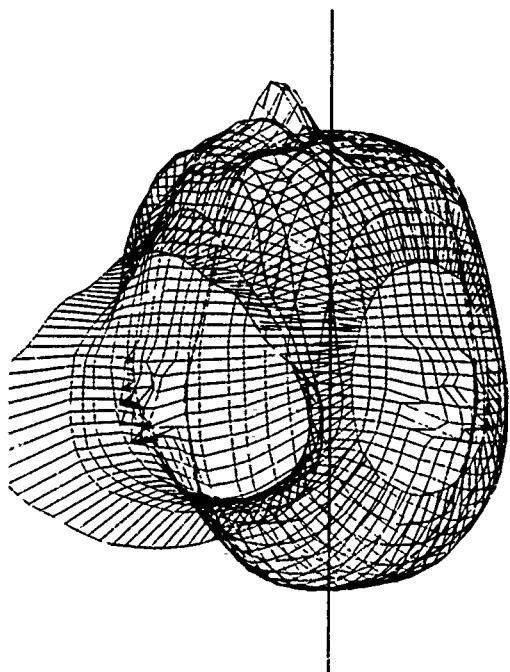
+20°



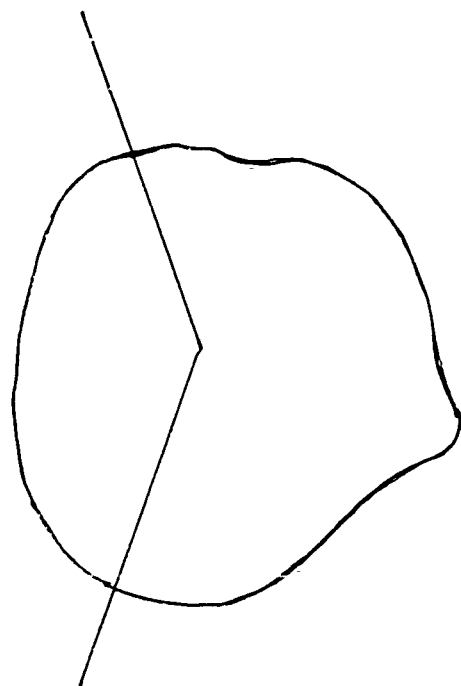
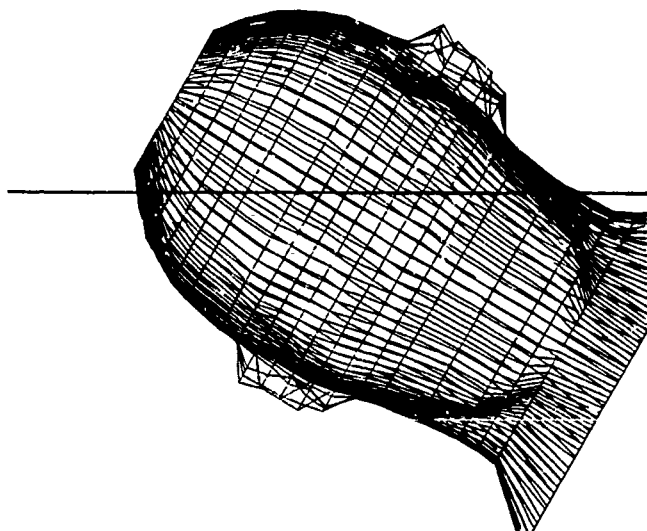


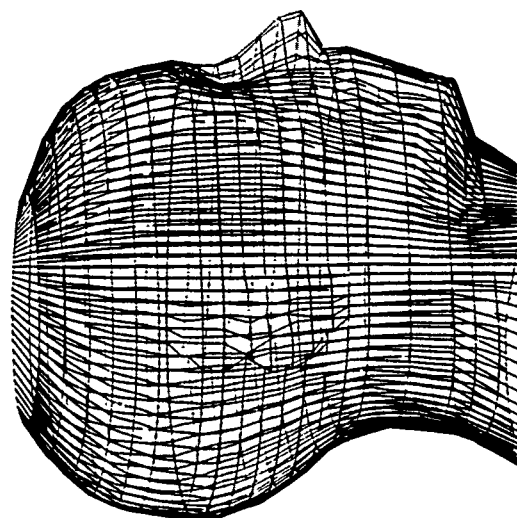
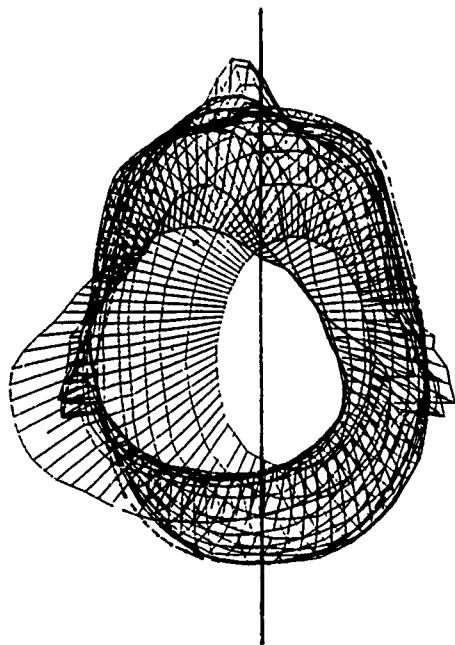
+40°



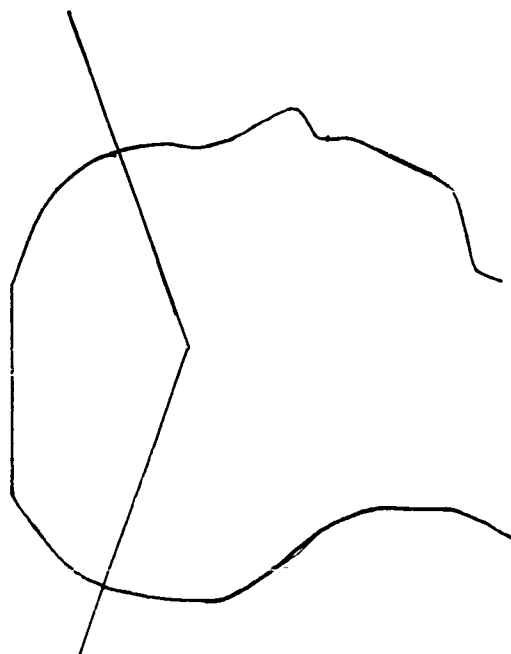
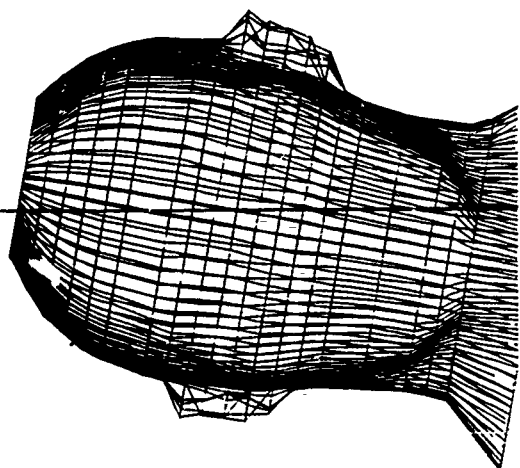


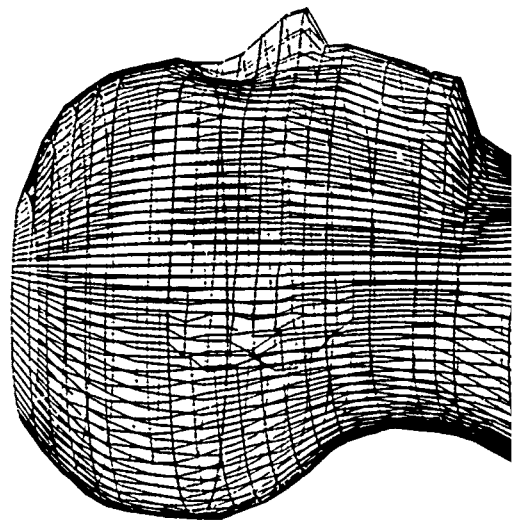
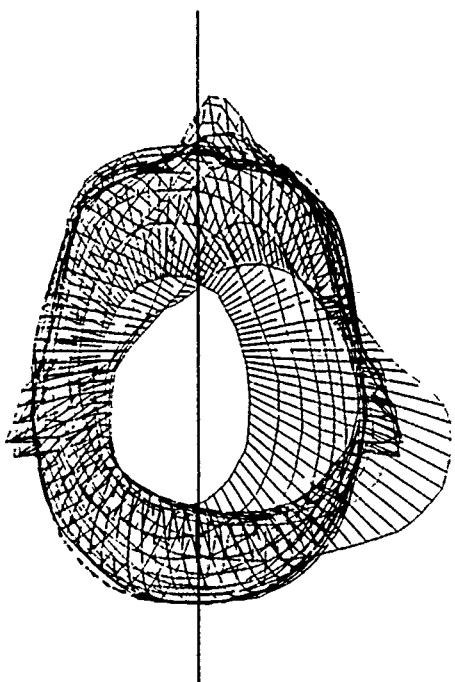
+ 60°



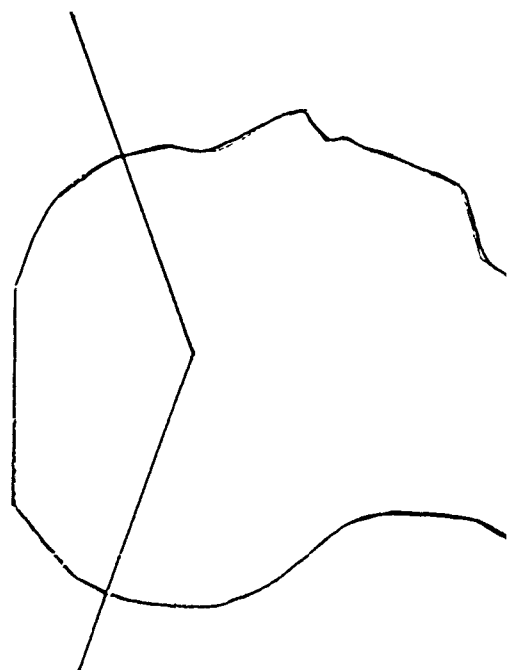
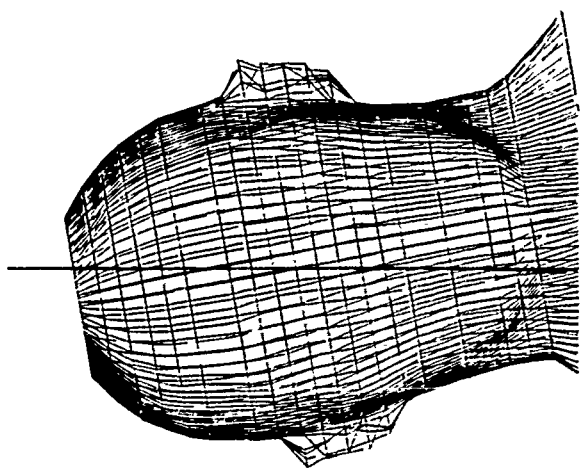


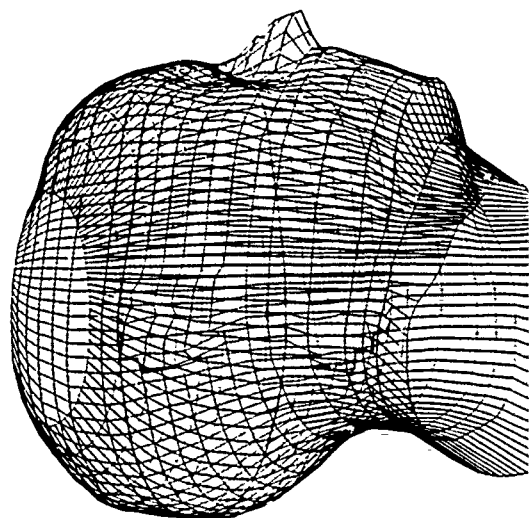
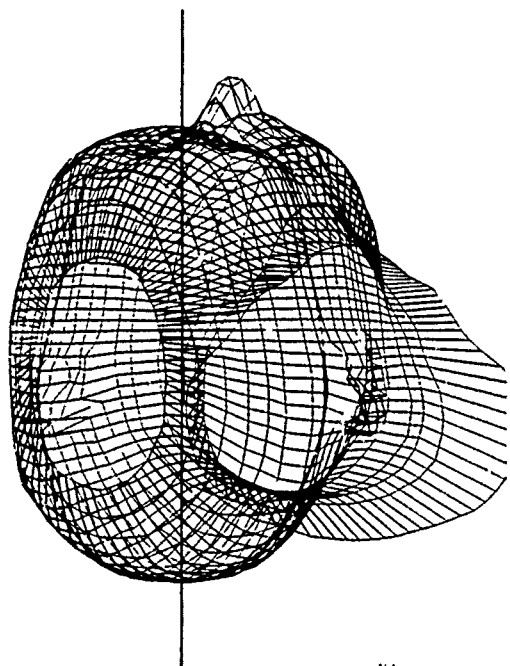
+80°



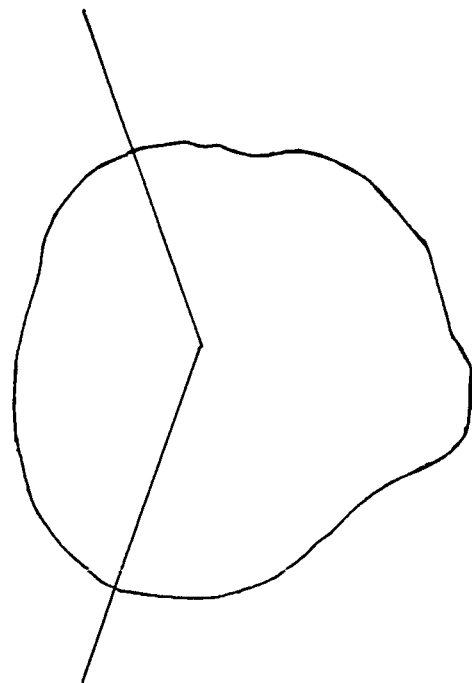
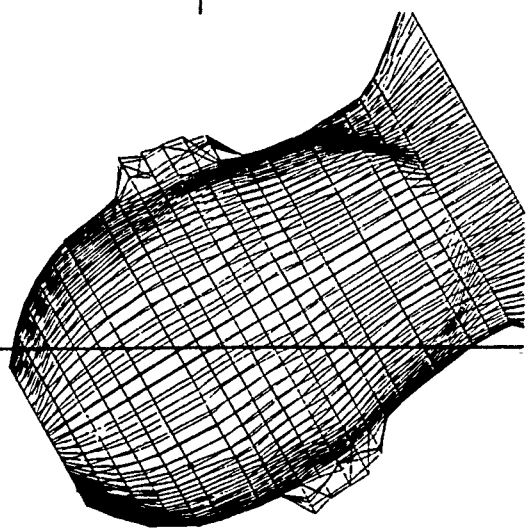


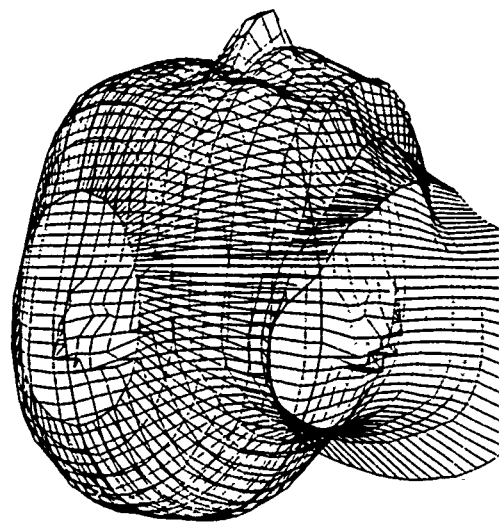
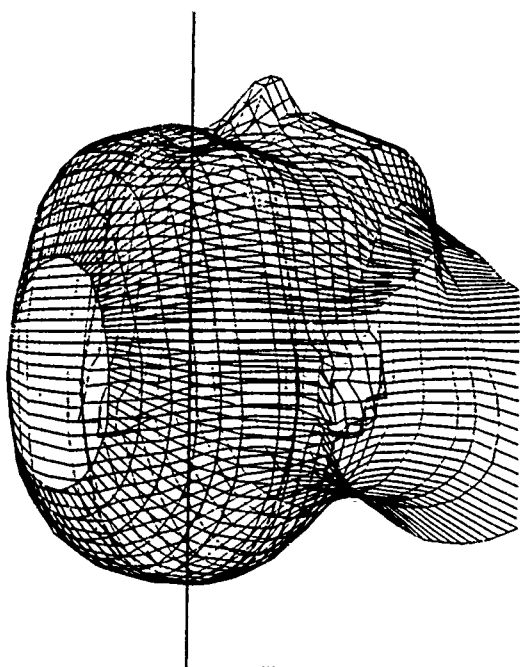
$\pm 100^\circ$



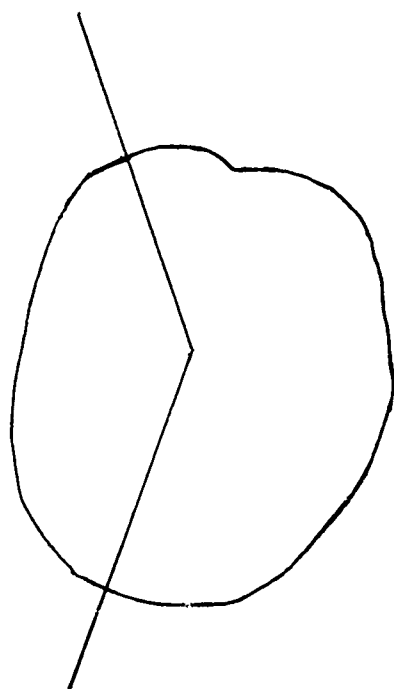
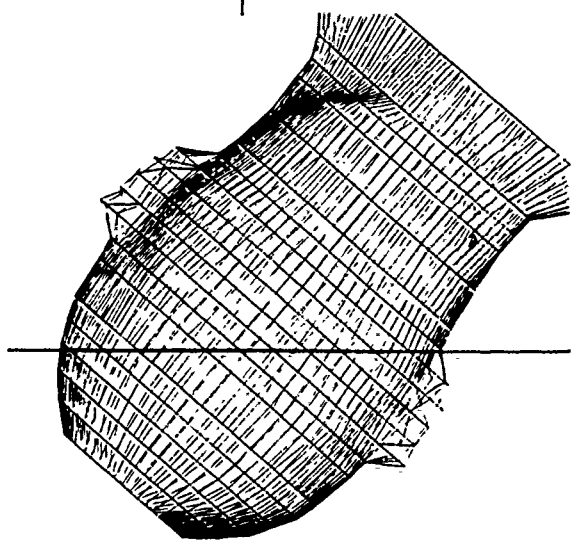


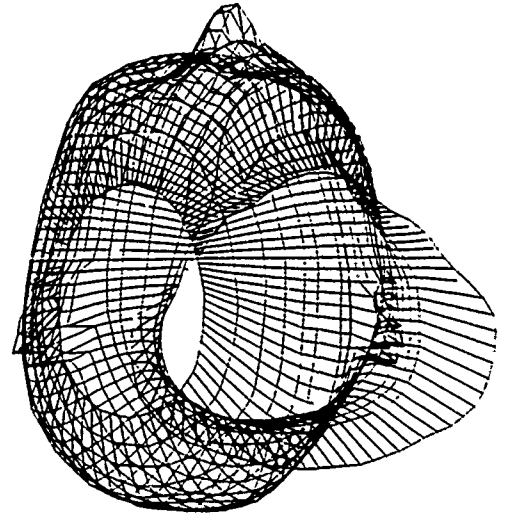
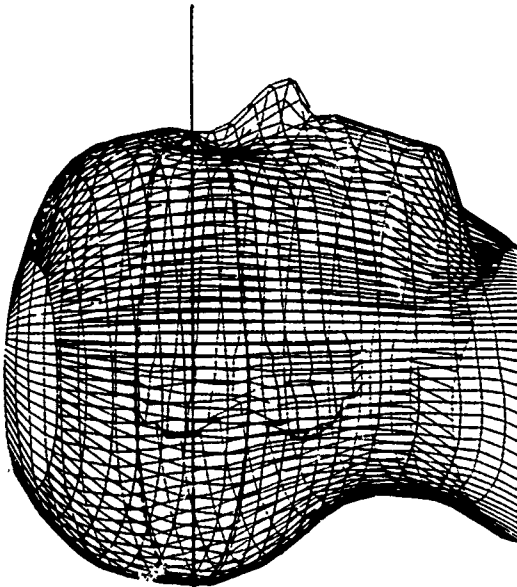
+120°



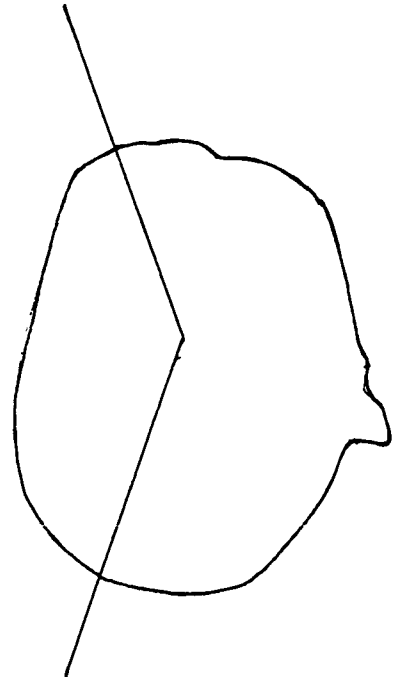
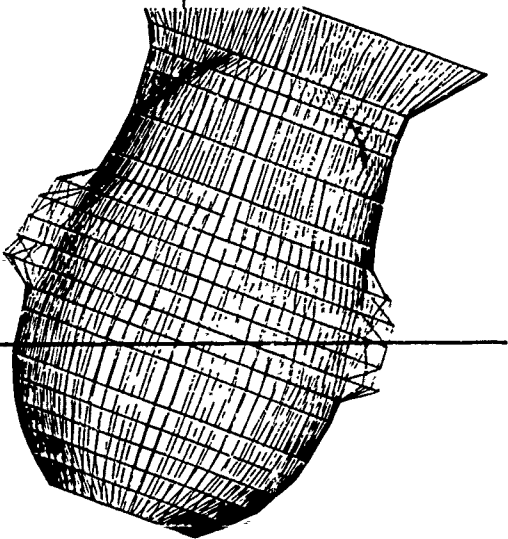


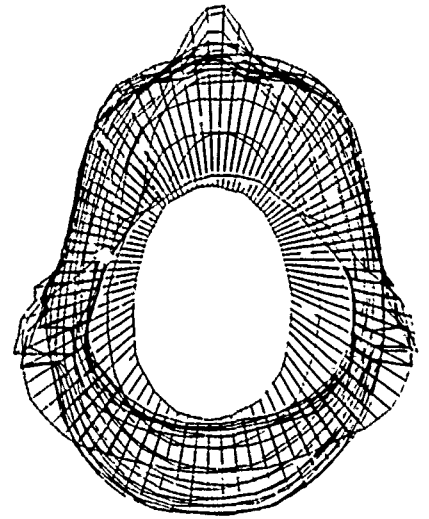
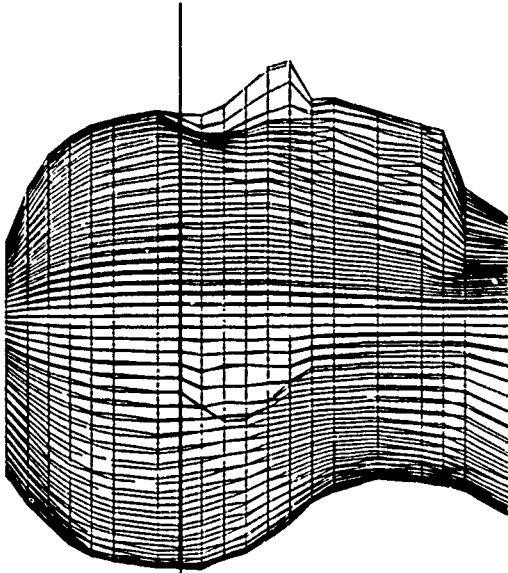
+140°



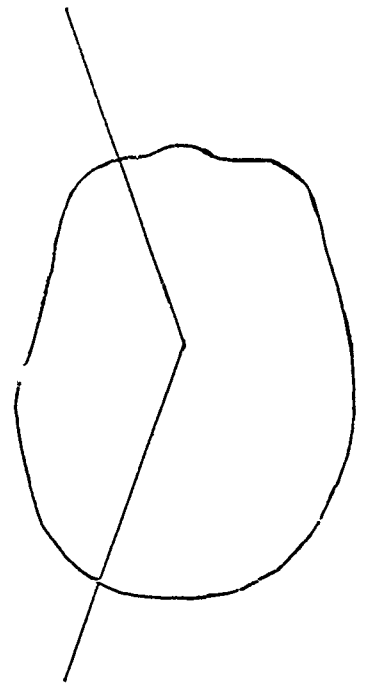
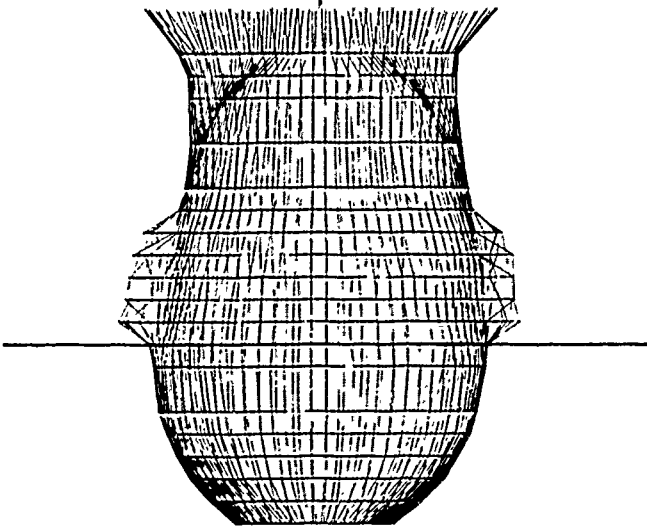


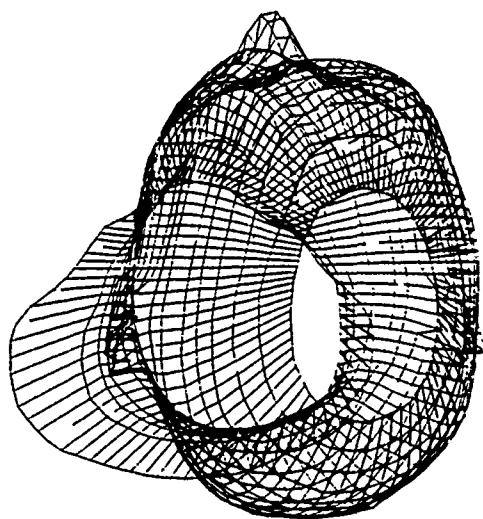
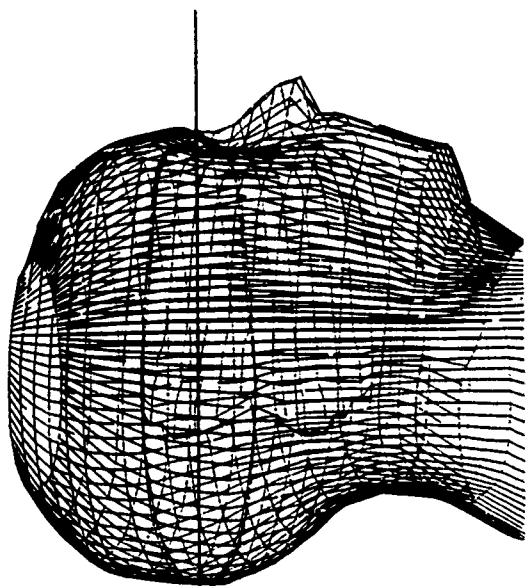
+160°



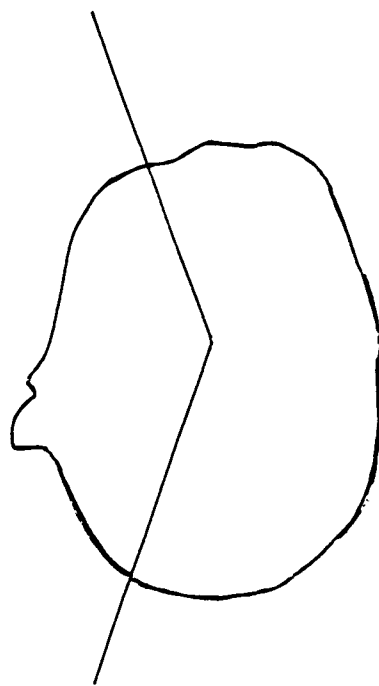
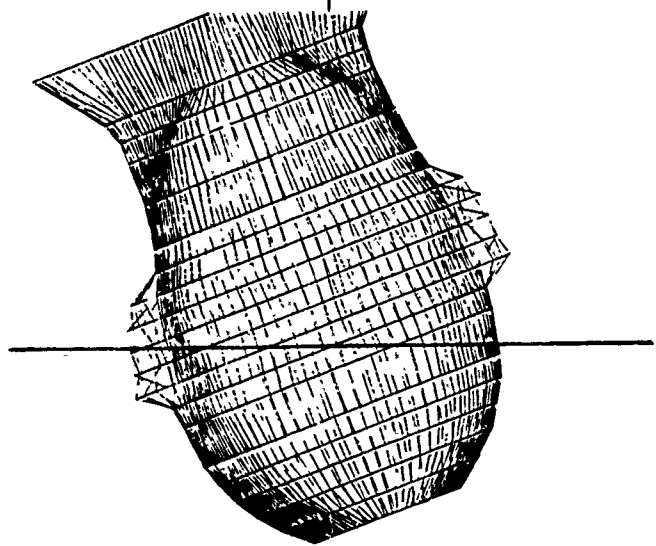


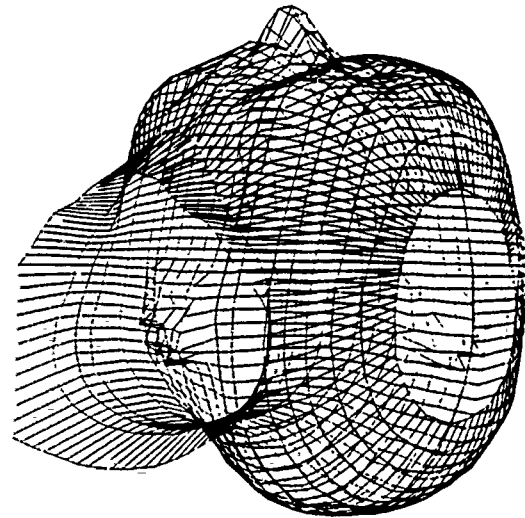
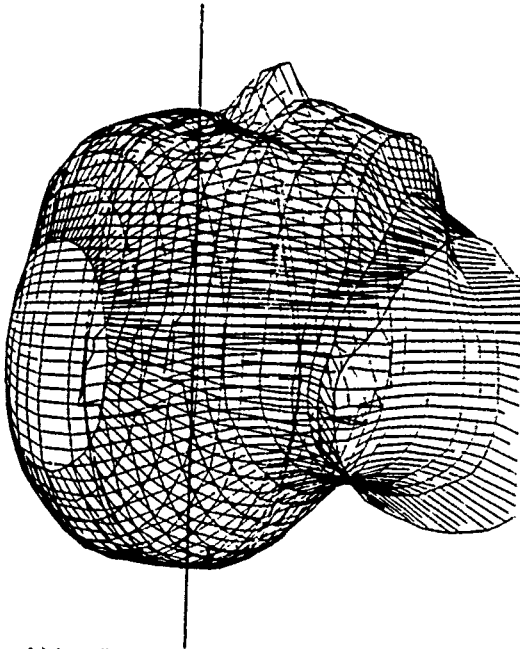
+ 180°





+200°





+220°

